RM-250

PHOTOMETRIC MEASUREMENTS OF SIMULATED LUNAR SURFACES

November 1964

Grumman

RESEARCH DEPARTMENT

GRUMMAN AIRCRAFT ENGINEERING CORPORATION

BETHPAGE NEW YORK

Grumman Research Department Memorandum RM-250

PHOTOMETRIC MEASUREMENTS OF SIMULATED LUNAR SURFACES

by

J. D. Halajian
Geo-Astrophysics Section

November 1964

Interim Report on NASA Contract No. NAS 9-3182

Approved by: Charles E. Mack, Jr.
Charles E. Mack, Jr.
Director of Research

SUMMARY

This report is in partial fulfillment of Contract No. NAS 9-3182 consisting of "Photometric Measurements of Simulated Lunar Surfaces."

All experiments in Phase I, consisting of photometric measurements at 0°, 30°, and 60° viewing angles on 23 specimens, have been essentially completed. The results of eight representative specimens are presented in this interim report. A description of the photometric analyzer, test procedures, and specimens, is followed by a discussion of test results, preliminary conclusions and recommendations.

The measured specimens include fine powders, coarse-grained volcanic ash, hard slags and scoria, etc. They all match the lunar curves at all viewing angles within the scatter of the lunar photometric data. The best fit is obtained by the "NASA slag." The results confirm previous findings with regard to the low albedo and high porosity of the lunar surface but go beyond them in indicating that it is no longer necessary to postulate a layer or veneer of fine dust on the moon in order to account for the lunar photometric data since these data are equally satisfied by "underdense-hard" materials that are just as likely to exist on the moon as fluffy dust.

TABLE OF CONTENTS

LIST OF ILLUSTRATIONS

INTRODUCTION

This is the first of two interim reports on the "Photometric Measurements of Simulated Lunar Surfaces" performed under Contract No. NAS 9-3182. This report covers parts of Phase I and Phase II of the contractual work as originally scheduled.

Phase I consists of photometric measurements at 0°, 30°, and 60° viewing angles of 18 promising specimens selected during preliminary Grumman funded photometric measurements at normal viewing angle only (Ref. 1). Five specimens, in addition to those specified in the contract, are also included at no additional cost. All specimens have been measured but only eight are presented in this report. That part of Phase II reported here consists of the preparation of samples only. Phase IIa experiments are currently being performed and will be presented in the next interim report.

Briefly, the purpose of the experiments in Phase I is to measure the backscattering properties of the selected specimens beyond a normal viewing position in order to establish as broad a match as possible with the lunar photometric data. The purpose of the succeeding experiments in Phases IIa and IIb is to evaluate the effect of the albedo, macroroughness, porosity and grain size on the photometric function by varying each variable more or less independently of the others and, possibly, to arrive at a quantitative relationship between these physical properties of the lunar surface.

The over-all purpose of the photometric investigations is to contribute to the definition of an "engineering" lunar surface model that is consistent with the material and environmental properties of the moon. The search for such a model may be conveniently started by establishing a large variety of photometric models and then narrowing these down in terms of the known polarimetric, thermal, and dielectric properties of the lunar surface. The validity of these models may also be assessed independently under simulated environmental conditions. Earth-based investigations of the moon could complement in a number of ways the mission of unmanned lunar probes in paving the way for manned landing

A description of the photometric test setup and procedure, and an account of refinements recently introduced into the photometer system are given after a brief review of current experimental work in lunar photometry. A tentative evaluation of the test results is submitted pending a more complete analysis to be given in the final report after the completion of Phases IIa and IIb.

CURRENT STATUS OF EXPERIMENTAL LUNAR PHOTOMETRY

The lunar photometric data are presently being utilized in engineering studies pertaining to visibility as well as to surface conditions of the moon. This investigation is oriented more toward the latter in an attempt to improve our knowledge of the physical and geometrical properties of the lunar surface which at the present cannot be readily obtained by other means. The facilities, techniques and models used in this connection may be equally useful to those interested in lunar visibility studies or simulation.

The most recent contributors to the field of lunar photometry are van Diggelen (Ref. 2) and Hapke (Ref. 3). A detailed review of their contributions as well as of their predecessors' will be given in the final report in order to present this work in its proper perspective.

It is briefly noted, however, that this work has been largely motivated by the paucity of known models which reproduce the lunar photometric curves and the notion that this could be due to the limitation of instruments used in "model-matching" experiments despite notable theoretical progress made in understanding the lunar photometric function.

It is known that common terrestrial rocks and soils do not backscatter light like the moon because they lack a sufficiently intricate structure. To date, the best known models that reproduce the lunation curves are materials of microscopic complexity such as van Diggelen's "Cladonia Rangiferina," a variety of lichen, and Hapke's "fairy castles," produced by loosely sifted micron-size dust particles. These models, and supporting theoretical estimates, suggest that a low albedo and high porosity ("with interconnected cavities") of the order of 10% and 80% respectively, are the most significant properties of a material which backscatters light like the moon. As a result of these theoretical and experimental studies, it was estimated that the photometrically relevant properties of a specimen are not peculiar to lichen or fine dust alone, but could be possessed by "macrorough," cohesive materials provided they are examined by a correspondingly large photometer capable of "seeing" a sufficiently large area containing a representative number of surface irregularities and shadows. Consequently, a photometric analyzer with an area viewing capability about an order of magnitude larger than that viewed by a previous instrument was built at

Grumman in order to examine theoretically promising specimens (such as volcanic ash and scoria) which were previously rejected as unsuitable.

The Grumman photometer, the samples used, measurement techniques and results are described in the following sections.

TEST EQUIPMENT

Prior to the inception of the contractual photometric program, a series of other Grumman funded studies were conducted, using the photometric analyzer. As the studies progressed, improvements were incorporated into the equipment with a consequent refinement of the method of obtaining and recording the data. It was, therefore, necessary to repeat all of the original investigations (at no additional cost to the contract) and incorporate them herein. Only slight differences are discernible in the original and recent data, with the latter being more reliable in all cases. Some of the improvements are described in this report.

As shown in Figs. 1 and 2 the device simulates the sun-moon-earth optical relationship. The sun is simulated by a collimated source. It is mounted on a counterbalanced rotating arm, approximately 8 feet from the sample. At the center of rotation, the sample simulates a portion of the lunar surface; the table on which it rests can be tilted to change the viewing angle. The table can be adjusted vertically to assure that the light is always beamed to the same part of the sample. The electronic photometer, mounted on the ceiling, views the sample as a similar instrument would view the moon from the earth. The phase angle of the actual sun-moon-earth geometry can be set up by rotating the sun source. Two additional photometers at 30° and 60° viewing angles have been mounted on the ceiling not only for convenience but also to obviate the necessity of tilting the sample table and the possibility of disturbing particulate specimens.

Some of the unique capabilities of this photometric analyzer are:

1. To read at zero and near-zero phase angles. This is accomplished by means of a "beam splitter" which, at phase angles other than zero (or near zero), is replaced by a first-surface mirror to assure a source of unpolarized light to and from the sample. At small phase angles, the polarization produced by the beam splitter is negligible.

2. To plot automatically the photometric curve as the light source swings over the sample.

3. To take polarimetric readings. This is accomplished by means of a rotating polarizing filter (polaroid) mounted in front of the "normal" photometer at the various positions of the sun source.

4. To sample large areas. This capability assures meaningful data from surfaces having large-scale irregularities, i.e., mm to cm. Presently, 3-inch diameter areas can be measured. This capability could be expanded to 12 inches or more; the limit is established by the physical dimensions of the facility. Focused light may be used in place of collimated light for very large, less precise work.

The objective lenses for the photometers and sun source are twelve inch f 2.5 units used in the K-37 camera; the camera bodies are also used.

The sun source and polarizer are motor driven and controlled at a single panel, from which the selection of one of the three photometers can also be made. The three photometers may be seen in Fig. 1. Only the photometer with a zero degree viewing angle is equipped with the polarizer.

Crossed axes front surface mirrors are used with the sun source to eliminate polarization bias in the light received by the specimen. At a zero degree phase angle, a beam splitter is substituted for the second mirror.

The following features of the Grumman Photometric Analyzer assure accurate and repeatable photometric measurements.

1. The light is well collimated, allowing the formation of sharp shadows. The angular size of the sun (30 minutes of arc) is duplicated in the collimated source, so that the shadowing is more realistic. The sun source is made uniform by the use of diffuser disks.

2. Considerable care is taken to minimize extraneous scattered light which could seriously prejudice the results. The equipment is operated in a darkened room. Were the source modulated, some low level illumination would be permissible, but the

scatter of modulated light from the source itself would require close attention. In a darkened room, undesirable scatter can be observed and corrected for.

3. The illuminated portion of the sample is slightly less than 4 inches in diameter. This is sufficiently large to assure an integration of the effect of the macrostructure of the coarsest specimen used, such as slag, volcanic ash, meteorites, etc.

4. Each of the three photometers is equipped with a field stop which carefully and definitely limits the viewed area to a disk within the perimeter of the illuminated area. Viewing of the natural boundaries or edges of the specimens is avoided. The viewed area is carefully centered on the axis of rotation of the sun source so that the center of the illuminated disk does not shift as the arm supporting the sun source is rotated. Keeping the photometers static while rotating the sun source permits the examination of particulate materials that remains undisturbed throughout the test.

5. With the use of large receiver optics, the light collection efficiency is high and the signal-to-noise ratio in the phototube output is optimal. The use of a tungsten-iodine lamp with a high intensity, behind the diffuser disk, also favors an excellent signal-to-noise ratio. The coplanar recorder is operated at a high gain to minimize the servo error. Some slight servo "jitter" of the recorder is evident, but insufficient to impair its accuracy. The use of a multiplier phototube (931A) is also conducive to an excellent signal.

6. The combination of the tungsten-iodine source (operating in excess of 3000°K) and a blue sensitive S-4 phototube, resembles the spectral response of lunar photographic photometry. The spectral reflectance of the materials involved is expected to be a minor factor of the visual photometric function.

7. The alignment of the sun source and the receivers (photometers) relative to the specimens, is carefully adjusted and periodically checked by optical techniques. The performance of the entire system is calibrated regularly by using standard samples with stable, known, characteristics. The error of the data can be shown to be less than two per cent for low albedo materials.

TEST PROCEDURE

The initial step with all of the photometric tests, following the sample preparation, is to position the specimen properly on its stand. It is aligned in a manner which permits all of the photometers to view the same illuminated disk, never an edge of the specimen or the stand itself. A thin veneer of powder or a thick rock specimen is accommodated by raising or lowering the stand so as to leave the upper surface of the specimen at the same level.

With the sun source extinguished, the arm is rotated in a totally dark room, thereby producing a horizontal trace on the two axis recorder, representing the dark current level. The operation is repeated with the sun source turned on, to adjust the gain of the photometer so that the output above the dark current level may be normalized to a standard reference point in the lunation curve. The photometric curve is then taken with the front surface metal mirrors through the complete rotation of the sun source. The second mirror is then replaced by the beam splitter. The curve is then completed through the previously eclipsed nine degrees of arc.

In succession, the 30° and 60° photometers are used to plot the reflectivity of the undisturbed specimen. The mirrors and the beam splitter are carefully cleaned at each removal or replacement. Light reflected by the beam splitter to the wall is trapped by a drape of black flock cloth* to prevent a secondary reflection from this source.

The test curves are automatically plotted on a recorder as the sun source is rotated throughout a full lunation. When the specimen curves have been completed, a plastic template for each corresponding standard lunation curve is matched to it at the previously established normalization point, and the lunar curve is drawn in.

*Synthon Inc., Cambridge, Mass.

STANDARD LUNATION CURVES

The standard lunation curves of van Diggelen (Ref. 2) are used in this report as a basis of comparison with the test curves. These curves have also been used by Hapke (Ref. 3). The 0°, 30°, and 60° standard curves correspond to the 0-10°, 30-50°, and 50-90° crescents of van Diggelen as shown in Fig. 3 (Ref. 2). The points in this figure represent the lunation curves of individual craters on the moon and reveal an appreciable scatter. No attempt was made to interpolate lunation curves from the van Diggelen standard for actual 30° and 60° longitudes to correspond to the fixed location of our photometers. The slight change that such an interpolation would introduce is probably within the scatter of the lunar data. This interpolation will be done in a future report and the results will be compared with other published lunar standards (particularly those of Orlova for the lunar highlands and lowlands) in order to establish a lunar photometric standard consisting of a "band" rather than a single line.

SAMPLE SELECTION AND PREPARATION

Phase I

The contractually required specimens were analyzed photometrically and albedos determined. They are listed as follows:

1. Silver Chloride (Aged)
2. Copper Oxide
3. Copper Oxide on Scoria No. 2
4. Volcanic Ash No. 1
5. Volcanic Ash No. 2
6. Volcanic Ash No. 3
7. NASA Slag (Smooth)
8. NASA Slag (Rough)
9. Copper Oxide on Slag
10. Foam
11. Silver Chloride (Aged) on Foam
12. Dendritic Copper
13. Meteorite (Imilac)
14. Meteorite (Krasnojarsk-896)
15. Coral No. 1
16. Coral No. 2
17. Coral No. 3
18. Coral No. 4

In addition, a number of noncontractual specimens were also investigated at no additional cost.

19. Carborundum
20. Leveled NASA Slag (Rough)
21. Meteorite (Krasnojarsk-897)
22. Scoria No. 1
23. Scoria No. 2

The silver chloride, copper oxide and carborundum are fine powders (less than .037 mm). All powders were lightly sifted through a 400 mesh screen onto a flat, smooth, board for a minimum thickness of 2 mm. The silver chloride specimen was then darkened by exposing it to sunlight, modifying the surface to an oxide and possibly some free silver.

The volcanic ash (Fig. 7d) consists of porous particles predominantly of centimeter size. The exact distribution of particle size will be determined and incorporated into a future report.

The "NASA slag," shown in Fig. 8d, is a solid slab of complex textured furnace slag (1/8 to 1/4 inch angular projections and interconnected cavities) having a fairly flat surface on one side, referred to as "smooth," and a slightly more irregular, knobby surface on the other, termed "rough." Actually, both sides are equally rough. The wedge shape of the slab accounts for the asymmetrical curve of the "rough side." When leveled, some symmetry was restored.

A composite model was created by sifting the same copper oxide powder used in specimen 2 onto the flat NASA furnace slag, number 7.

The foam (specimen 10) is a dark, flexible, polyurethane foam, plucked to give it an irregular surface. A composite model was created by sifting the silver chloride (specimen 1) upon it, and aging it in sunlight.

The original dendritic copper was lost and replaced with a somewhat less dendritic specimen of native copper as shown in Fig. 13. The meteorites are all pallasites, including the Imilac shown in Fig. 9d.

Except for coral number 1, which has been slightly darkened, all are natural coral specimens. Coral number 2 is shown in Fig. 10d.

The scoria specimens shown in Fig. 11d are almost identical slabs having closed vesicules with a depth to diameter ratio of two to one. Scoria number 1 is slightly darker than number 2.

Phase II

As described in the contract, Phase II consists of examining composite specimens of simple geometric forms with a surface of fine dark powder.

The geometric forms have been made from wood and the powder is essentially the copper oxide of Phase I, sifted through a 400 mesh screen. Although the forms have been prepared, the photometric measurements have not been made, but are expected to be reported on in the next interim report.

DATA PRESENTATION

In the early photometric studies conducted by Grumman, the lunar and specimen reflectivity curves were normalized at a zero degree phase angle. This representation was possible because the use of the beam splitter enabled us to obtain data at zero degrees.

A re-evaluation of the test curves produced by us and by others revealed that a more realistic point at which the lunar and test curves could be normalized is the "near eclipse" point since the reflectivity of the moon at this point is known whereas at zero phase it is not. It was decided therefore to rerun all the curves by normalizing them at the point where the beam splitter obscures the samples. This point is about at $\pm 4.5^\circ$ phase.

So far, eight specimens have been rerun with the normalization point below the extrapolated peak. They are:

1.	Silver Chloride (Aged)	Specimen No. 1	Fig. 5
2.	Copper Oxide	Specimen No. 2	Fig. 6
3.	Volcanic Ash No. 3	Specimen No. 6	Fig. 7
4.	NASA Slag (Level, Rough)	Specimen No. 20	Fig. 8
5.	Imilac	Specimen No. 13	Fig. 9
6.	Coral No. 2	Specimen No. 16	Fig. 10
7.	Scoria No. 1	Specimen No. 22	Fig. 11
8.	Scoria No. 2	Specimen No. 23	Fig. 12

The remaining curves will be submitted in the next interim report.

DISCUSSION OF TEST RESULTS

The results of the photometric measurements are shown in Figs. 5 to 12. The standard lunation curves used for comparison with the test curves are those of van Diggelen (Ref. 2) shown in Fig. 3. Albedo values accompany the test curves.

A preliminary study of the current results suggest some conclusions, some of which have been found by other investigators. Briefly, the following remarks could be made at this time:

1. All the specimens show a maximum radiance at zero phase angle (corresponding to full moon) independent of the viewing angle (or location on the moon). This photometric peculiarity of the moon was first discovered by Barabashev (Ref. 4) and is obeyed by all the specimens we have selected. In no case was a shift in phase noticed, that is to say, a lag between zero phase (full moon) and maximum radiance, as reported by van Diggelen (Ref. 2) for some of the rayed craters shown in Fig. 4. It may be pertinent to note that Gehrels'* recent

*University of Arizona, Lunar and Planetary Laboratory

observation of these craters (unpublished data), like our own measurements of laboratory specimens, do not confirm this photometric anomaly reported by van Diggelen.

2. The zero phase peak of the specimens (made possible by means of the beam splitter) exceeds the extrapolated peak of the standard lunation curve within ±4.5° phase near eclipse. The lunar data in this region should remain suspect until more reliable measurements as close to eclipse as possible are taken. Gehrels' unpublished curves for particular areas of the moon reach closer to the zero phase point than previously published curves and show a tendency toward a sharper backscatter similar to our test curves. It would be interesting to compare Gehrels' curves (if and when they are published) with those of the specimens. For a meaningful comparison it would be necessary to make new measurements on the specimens at viewing angles corresponding to the longitudes of the particular areas observed by Gehrels.

3. The match between the test and lunar curves at larger phase angles is good for the 0° as well as for the 30° and 60°, particularly for the "NASA slag." The photometric properties of the "cohesive" models at larger viewing angles, unlike those of the AgCℓ and CuO powders, were unknown but appear to be equally good. The hard "NASA slag" and the coarse-grained volcanic ash reproduce the lunar curves as well as or better than the powder specimens at all viewing angles.

In evaluating the test results it would be useful to recall that what is being compared is the "detailed" photometry of small laboratory specimens with the "integrated" photometry of the moon representing an area orders of magnitude larger. The standard lunation curves of van Diggelen represent averages for crescents encompassing some 10° to 40° longitudes; as to the Orlava standards, they represent averages for the highlands or the maria. The lunation curves of individual areas on the moon reveal a sizable scatter when plotted with the average curves, as shown in Fig. 3. What is significant in the lunar standards is the fact

that in all cases they peak at or near zero phase and follow a consistently uniform trend at larger phase angles despite the scatter and regardless of location on the moon. The test curves should be assessed in the light of the scatter within the lunar data and the significant properties that are common to the photometric curves of individual lunar areas or standard averages. In this perspective most of the proposed specimens that were found promising on the basis of their good match at normal viewing angle (Ref. 1) reproduce the entire lunar data reasonably well.

The albedo of all the specimens showing a good fit with the lunar curve, except that of the coral, is of the same order of magnitude as that of the lunar surface. The good match with the coral could be explained by the fact that its high albedo is compensated by a high degree of complexity at both micro and macro scales.

The good results obtained with the hard NASA slag and coarse-grained volcanic ash are significant in as much as these models were investigated by others (Refs. 2 and 3) and rejected as unsuitable. It is apparent that neither a microrough structure nor a very low bearing strength are necessary conditions to reproduce the lunar photometric curves. The volcanic ash, in particular, is of particular interest because it is one of few materials reported by Dollfus (Ref. 5) to match closely the lunar polarization curve. It would be very desirable to measure the polarimetric and thermophysical properties of the Hawaiian volcanic ash, the NASA slag and other specimens of good photometric quality.

Van Diggelen measured the photometric properties of several specimens of volcanic ash. He found that their albedo was very close to that of the lunar craters but the shape of their photometric curves did not agree with those of the moon. As a result, he was led to conclude that "from a photometric point of view the lunar surface is in no case to be described as a plane layer covered by volcanic ashes." The results obtained with the Hawaiian volcanic ash render the above conclusion premature and stress the importance of adequate sample selection and instrumental refinements in model-matching experiments of this nature. The large area-viewing capability of the Grumman photometer was already mentioned as a pertinent factor. The influence of sample characteristics, such as grain size, albedo, porosity, roughness, will be investigated in Phase II.

The above discussion of test results is preliminary and incomplete. It is hoped that a more adequate and meaningful evaluation of the Phase I findings will be presented after the completion of Phase II.

CONCLUSIONS

Particulate and massive materials selected on the basis of their good match with the lunar photometric curve at normal viewing angle exhibit an equally reasonably good fit at 30° and 60° viewing angles.

The low albedo and high porosity that is common to nearly all the good photometric models confirm previous findings by others (notably by van Diggelen and Hapke) and indicate that the outermost layer of the moon, whatever its origin, is nearly uniformly covered by a dark disrupted and intricately vesicular or dendritic material. The albedo and porosity of the contending lunar models (of the order of 10% and 80% respectively) deviate considerably from those of common terrestrial soils and rocks but could be accounted for reasonably by the known peculiarities of the lunar environment (Ref. 6).

The differences in material composition, bearing strength, consistency, depth and scale of roughness between the good photometric models are equally instructive. They indicate that these properties are not very relevant photometrically, hence, they should not be inferred from the lunar photometric data.

The major significance of these findings is that it is no longer necessary to postulate a layer of fine dust on the moon in order to account for the lunar photometric data since these data appear to be equally satisfied by cohesive models such as slag and scoria. These materials are just as likely to exist on the moon as fine dust. Unfortunately, the lunar photometric data are inherently not capable of narrowing the considerable divergence in bearing strength that exists between the good models revealed by this and other investigations. However, the high porosity that is common to nearly all of these models could contribute to the solution of this problem when used in conjunction with the lunar thermal data as discussed in Ref. 6. It is hoped that a quantitative estimate of this porosity could be made in Phase II of this investigation.

RECOMMENDATIONS

Useful areas of further investigations have emerged from the Phase I experiments. Some of these are directly related to photometry, other areas involve the interpretation of the less explored regions of the lunar data.

Briefly, these areas involve the following experiments:

1. Measure the lunation curves of the existing specimens at viewing angles corresponding to the longitudes of the individual craters measured recently by Gehrels. Compare the curves with the Gehrels data (when they are published) particularly near the zero phase angles.

2. Measure the lunation curves of the existing specimens at discrete wavelengths ranging from near UV to near IR. Compare the curves with corresponding lunar data if and when such data become available.

3. Measure the polarimetric properties of the existing and other specimens. Determine material and geometrical properties that are polarimetrically relevant. This portion of the lunar data is one of the least explored and understood.

The above experiments could parallel or follow the present work. The measurement of thermophysical and dielectric properties is equally important and will be dealt with in future reports.

ACKNOWLEDGMENTS

The author wishes to express his grateful appreciation for the expert assistance of Mr. H. Hallock of the Servo-Engineering Department and of his equally dedicated assistants Mr. J. Grausaukas and Mr. D. Lamberty.

The author is equally indebted to Mr. S. Penn for his valuable assistance in the over-all execution of this project.

REFERENCES

1. Halajian, J.D., The Search for a Lunar Surface Model - Vol. I, (a proprietary preproposal study) Grumman Advanced Development Report 1964. Also presented in part at the Meeting of the Committee of Extra-terrestrial Resources in Golden, Colorado, April 1964, as: "Old and New Lunar Photometric Models and What They Mean."

2. van Diggelen, J., "Photometric Properties of Lunar Crater Floors," Recherche Astron. de l'Observ. d'Utrecht, XIV, 2, 1959.

3. Hapke, B., van Horn, H., Photometric Studies of Complex Surfaces with Applications to the Moon, Center for Radiophysics and Space Research, Cornell Univ. CRSR 139, 1963.

4. Barabashev, N.P., Astr. Nachz. 217, 445, 1922.

5. Dollfus, A., "The Polarization of Moonlight" in Physics and Astronomy of the Moon, edited by Z. Kopal, Academic Press, N.Y., 1962.

6. Halajian, J.D., The Case for a Cohesive Lunar Surface Model, Grumman Report ADR.04-04-64-2, presented at the N.Y. Academy of Sciences Meeting on "Geological Problems in Lunar Research," May 1964.

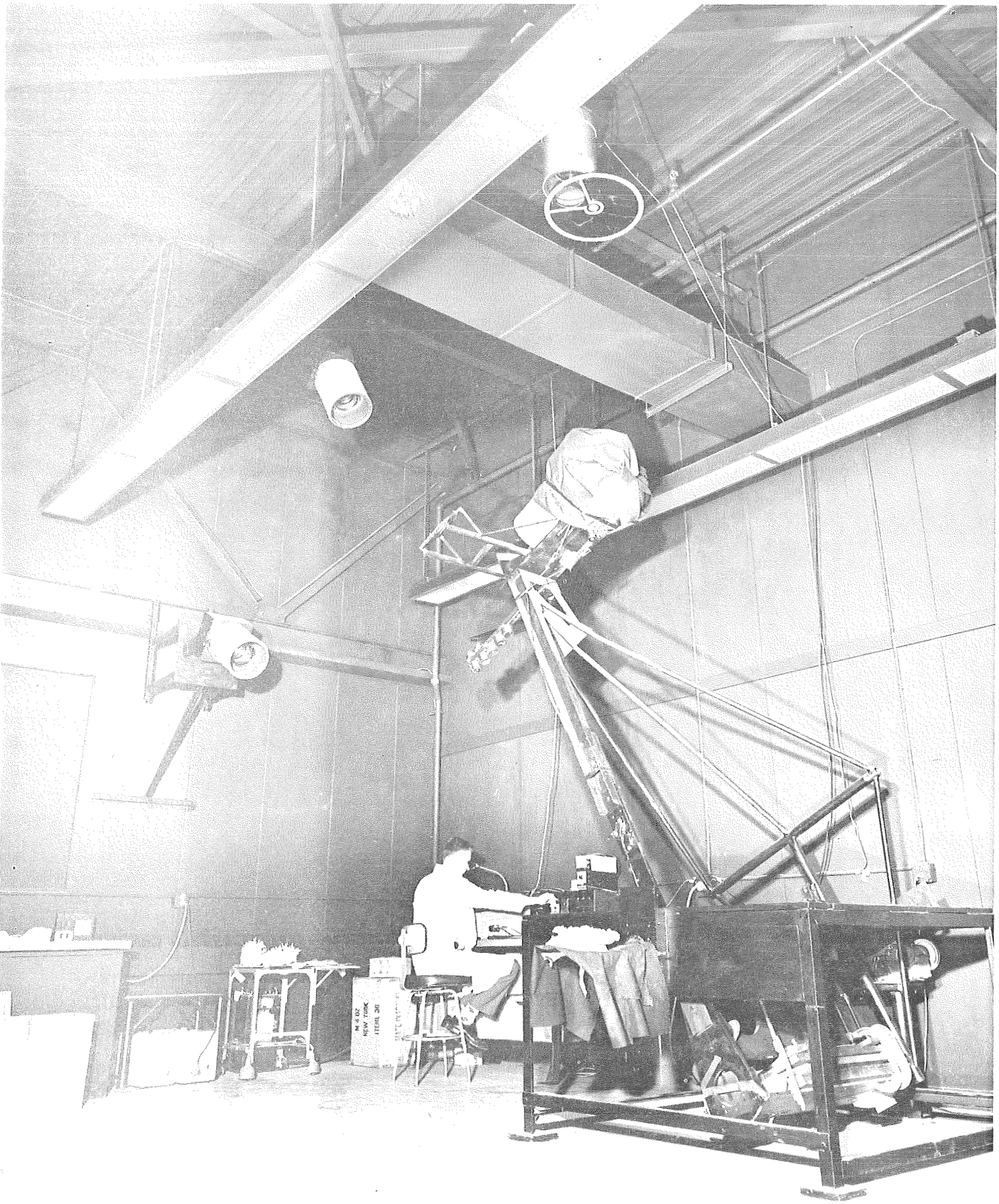

Fig. 1 Photograph of Photometric Analyzer

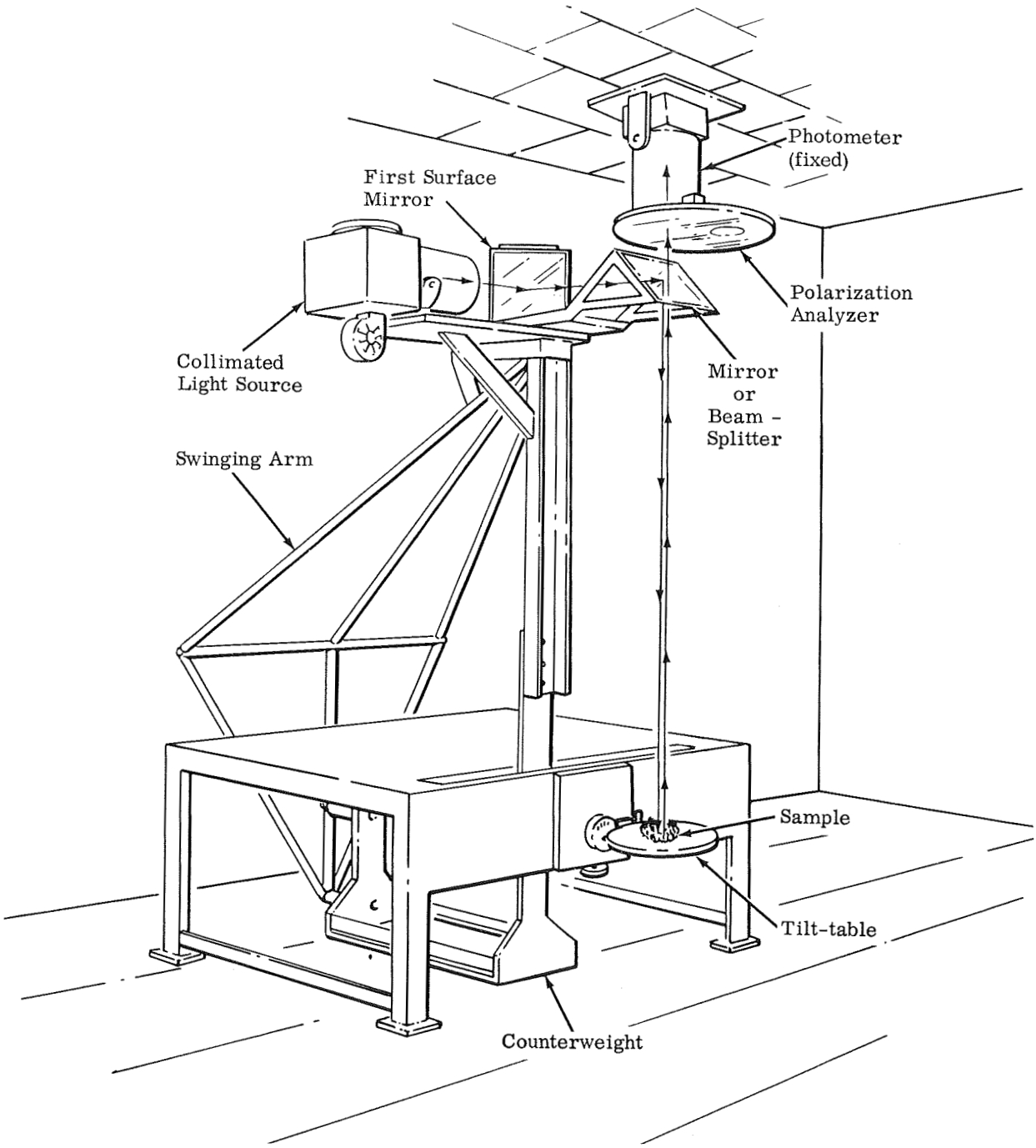

Fig. 2 Sketch of Grumman Photometric Analyzer
(30° & 60° Photometers Not Shown)

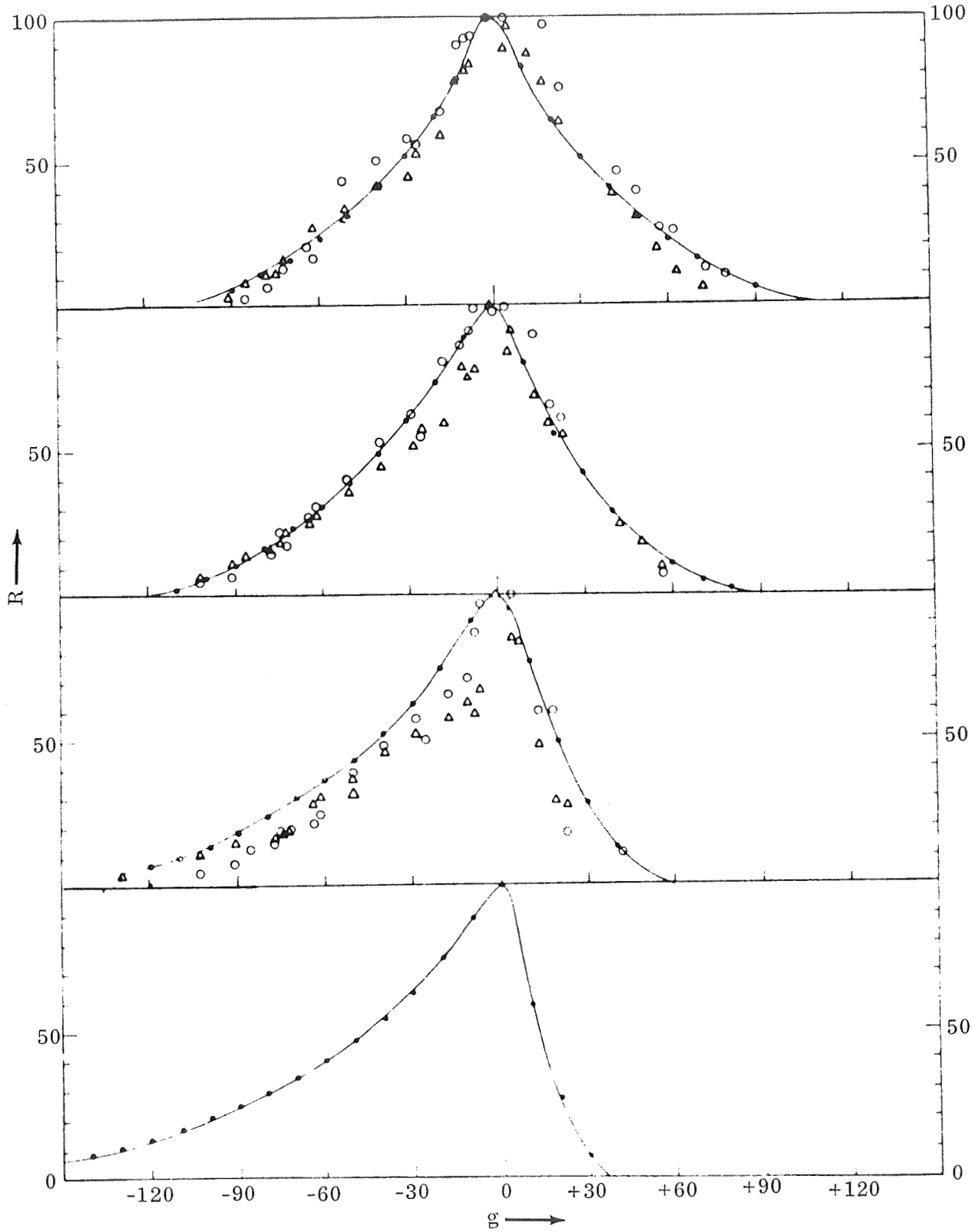

Figure 3. Van Diggelen's mean lunation curves of crater floors for four different crescents of selenographic longitude. Individual plains (Δ) and highlands (O) in the same crescent are measurements by Fedoretz. The four figures are related with:

1) Crescent λ 0 - 10, β 0 - 90
2) Crescent λ 10 - 30, β 0 - 90
3) Crescent λ 30 - 50, β 0 - 90
4) Crescent λ 50 - 90, β 0 - 90. Ref. (2).

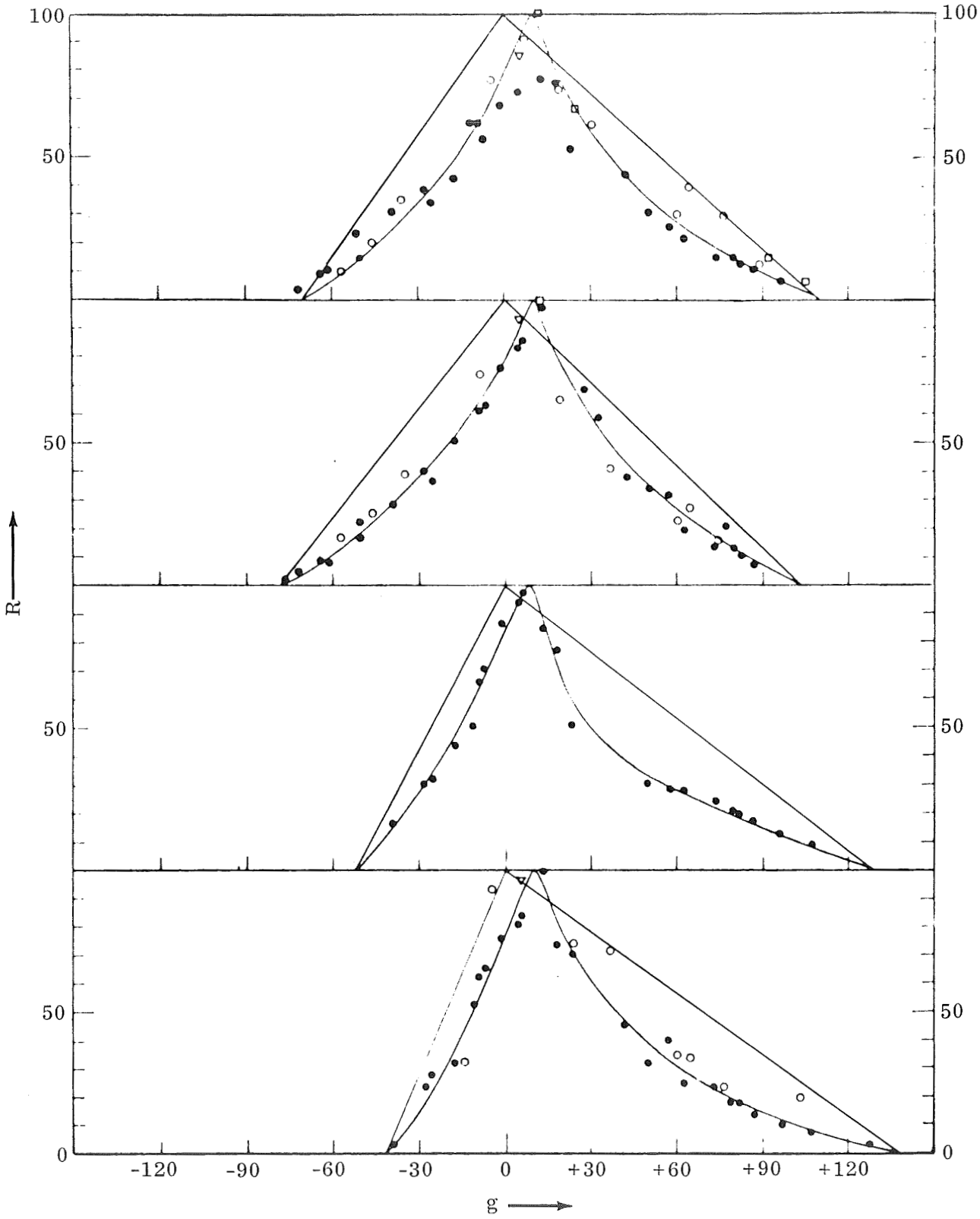

Figure 4. Lunation curves of four ray craters near the standard points. Copernicus, Tycho, Kepler and Aristarchus. The observers and the meaning of the marks is given in Ref. (2).

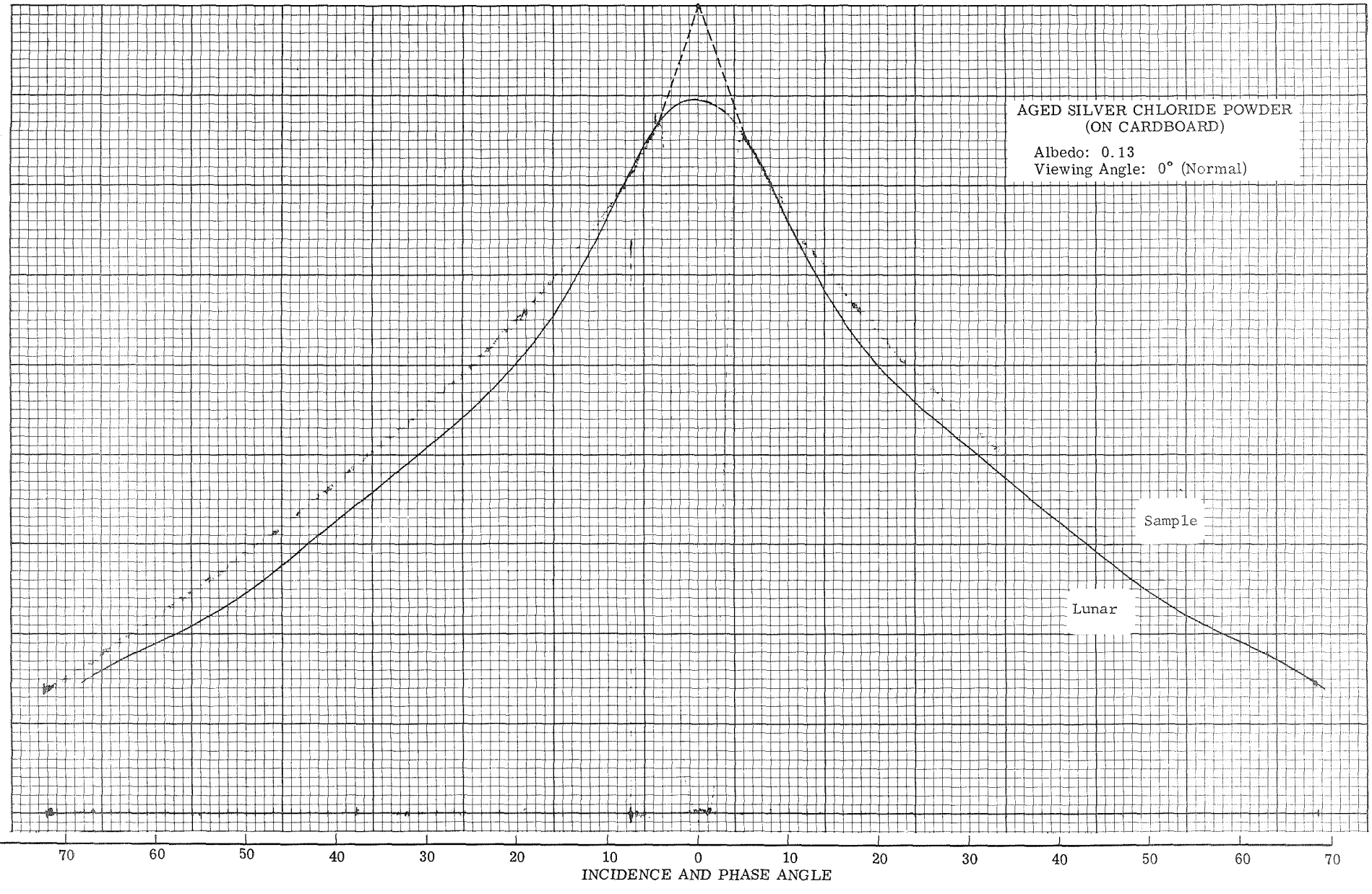
AGED SILVER CHLORIDE POWDER
(ON CARDBOARD)
Albedo: 0.13
Viewing Angle: 0° (Normal)
Sample
Lunar
80
70
60
50
40
30
20
10
0
10
20
30
40
50
60
70
INCIDENCE AND PHASE ANGLE

Figure 5a.

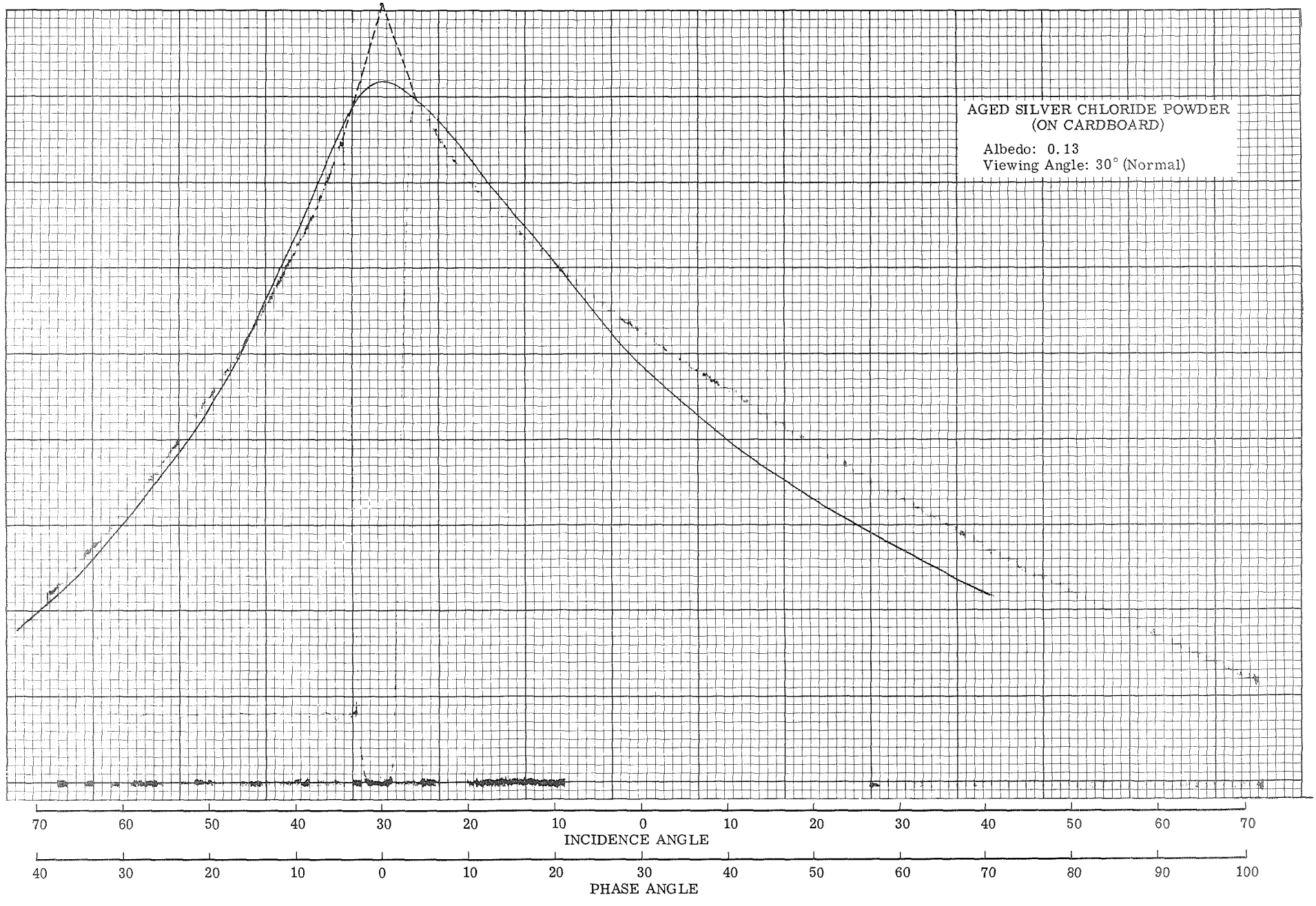
AGED SILVER CHLORIDE POWDER
(ON CARDBOARD)
Albedo: 0.13
Viewing Angle: 30° (Normal)
70 60 50 40 30 20 10 0 10 20 30 40 50 60 70
INCIDENCE ANGLE
40 30 20 10 0 10 20 30 40 50 60 70 80 90 100
PHASE ANGLE

Figure 5b.

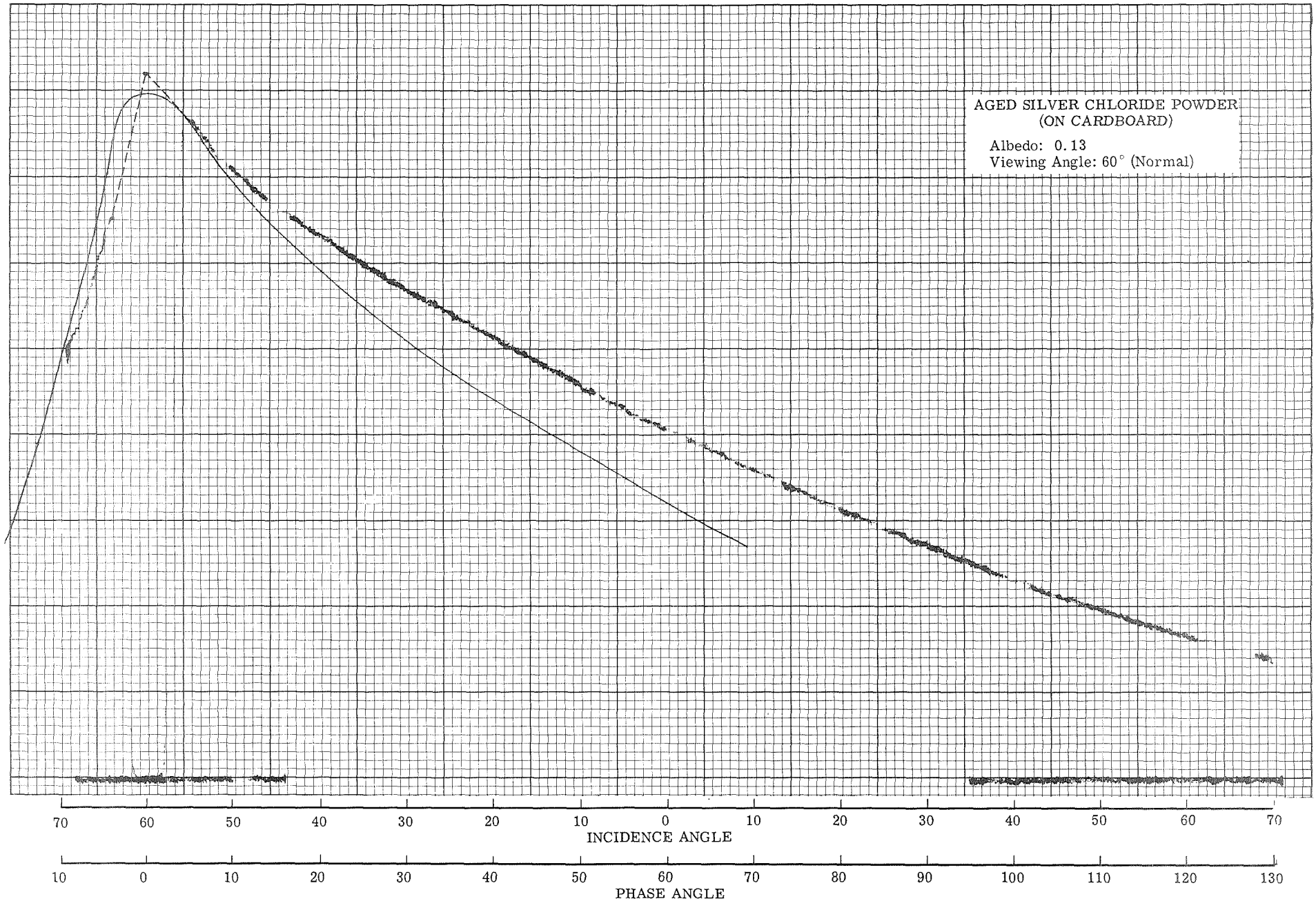
AGED SILVER CHLORIDE POWDER
(ON CARDBOARD)
Albedo: 0.13
Viewing Angle: 60° (Normal)
70 60 50 40 30 20 10 0 10 20 30 40 50 60 70
INCIDENCE ANGLE
10 0 10 20 30 40 50 60 70 80 90 100 110 120 130
PHASE ANGLE

Figure 5c.

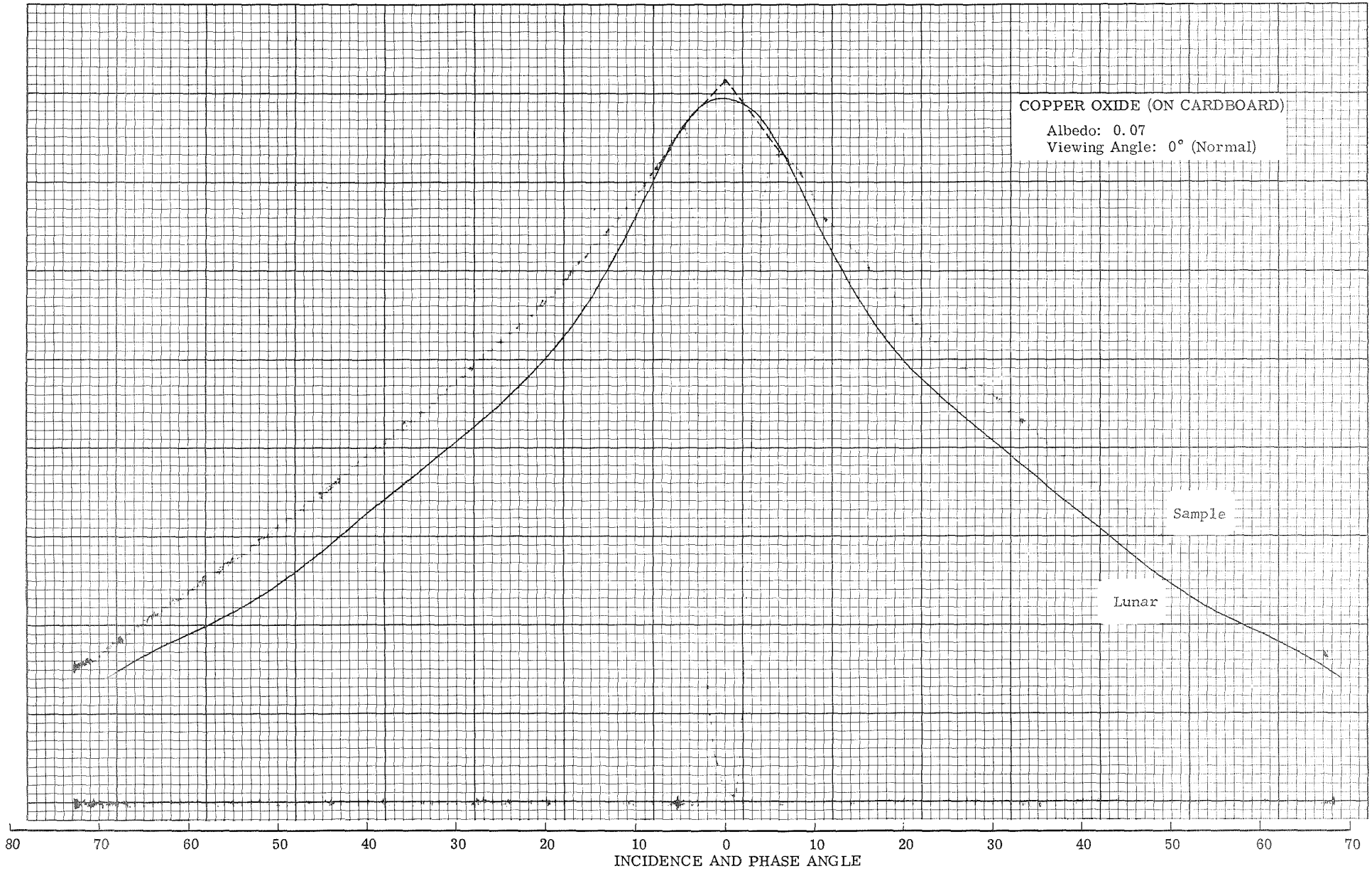
COPPER OXIDE (ON CARDBOARD)
Albedo: 0.07
Viewing Angle: 0° (Normal)
Sample
Lunar
80 70 60 50 40 30 20 10 0 10 20 30 40 50 60 70
INCIDENCE AND PHASE ANGLE

Figure 6a.

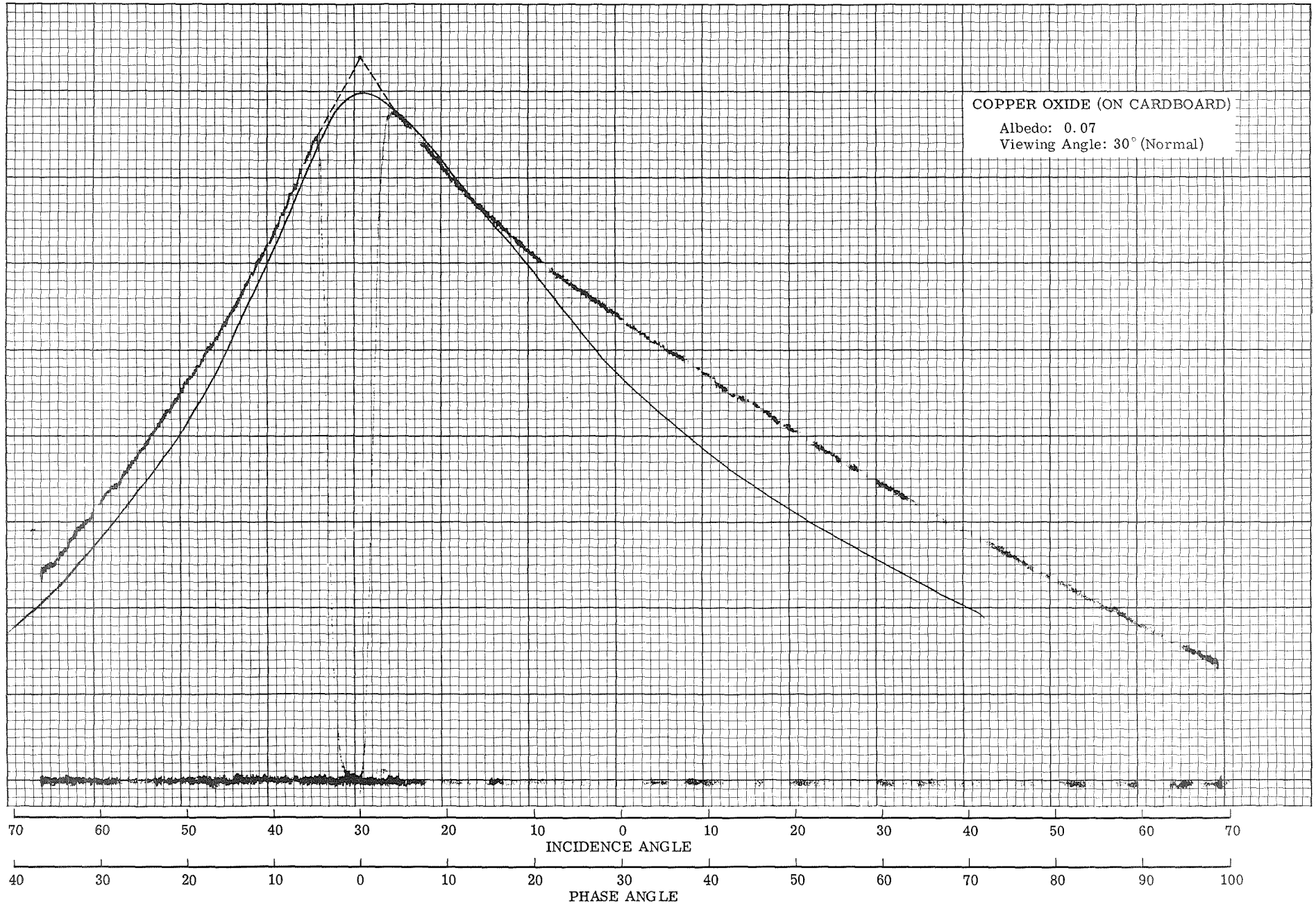
COPPER OXIDE (ON CARDBOARD)
Albedo: 0.07
Viewing Angle: 30° (Normal)
70 60 50 40 30 20 10 0 10 20 30 40 50 60 70
INCIDENCE ANGLE
40 30 20 10 0 10 20 30 40 50 60 70 80 90 100
PHASE ANGLE

Figure 6b.

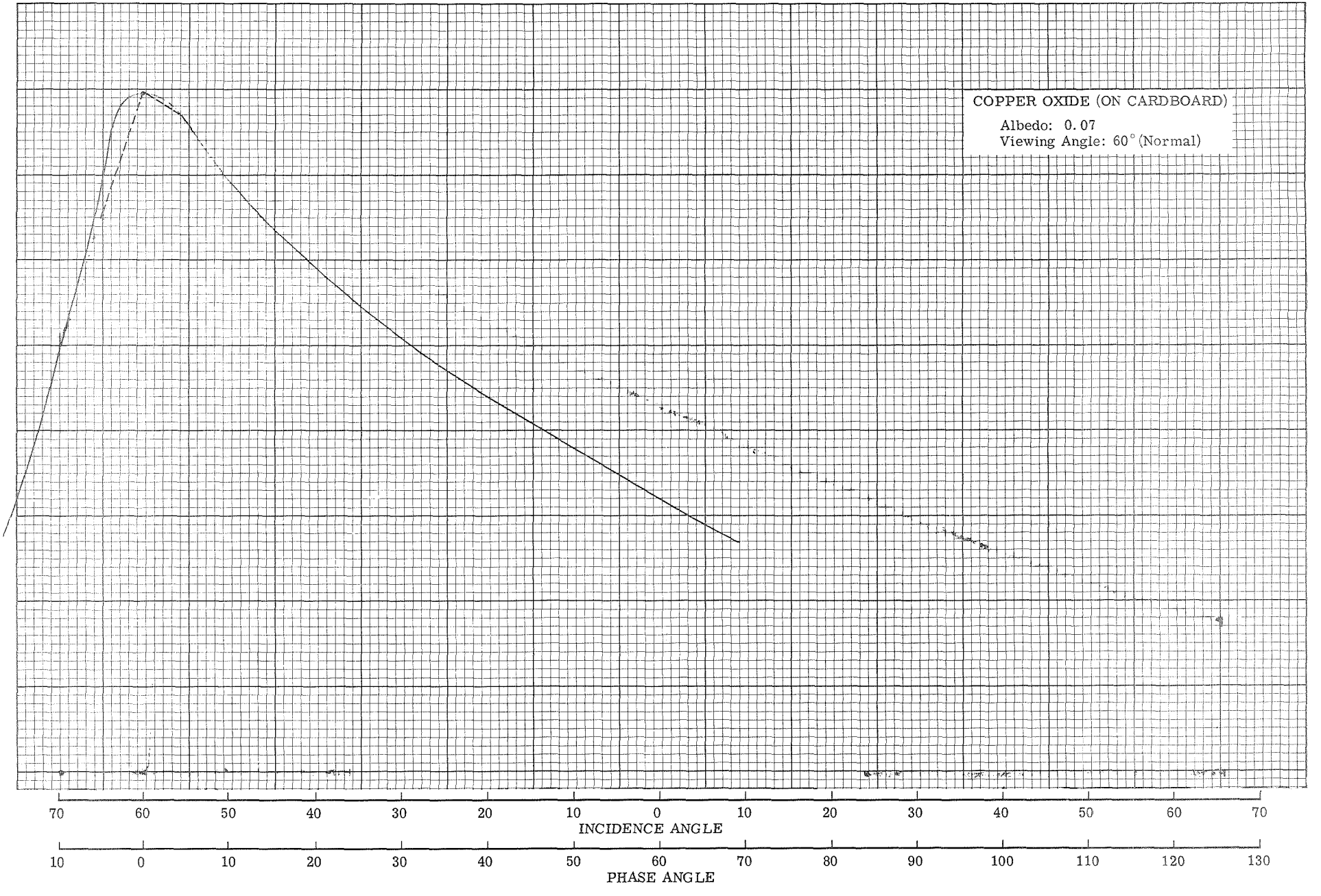

Figure 6c.

Research Dept.
RM-250
November 1964

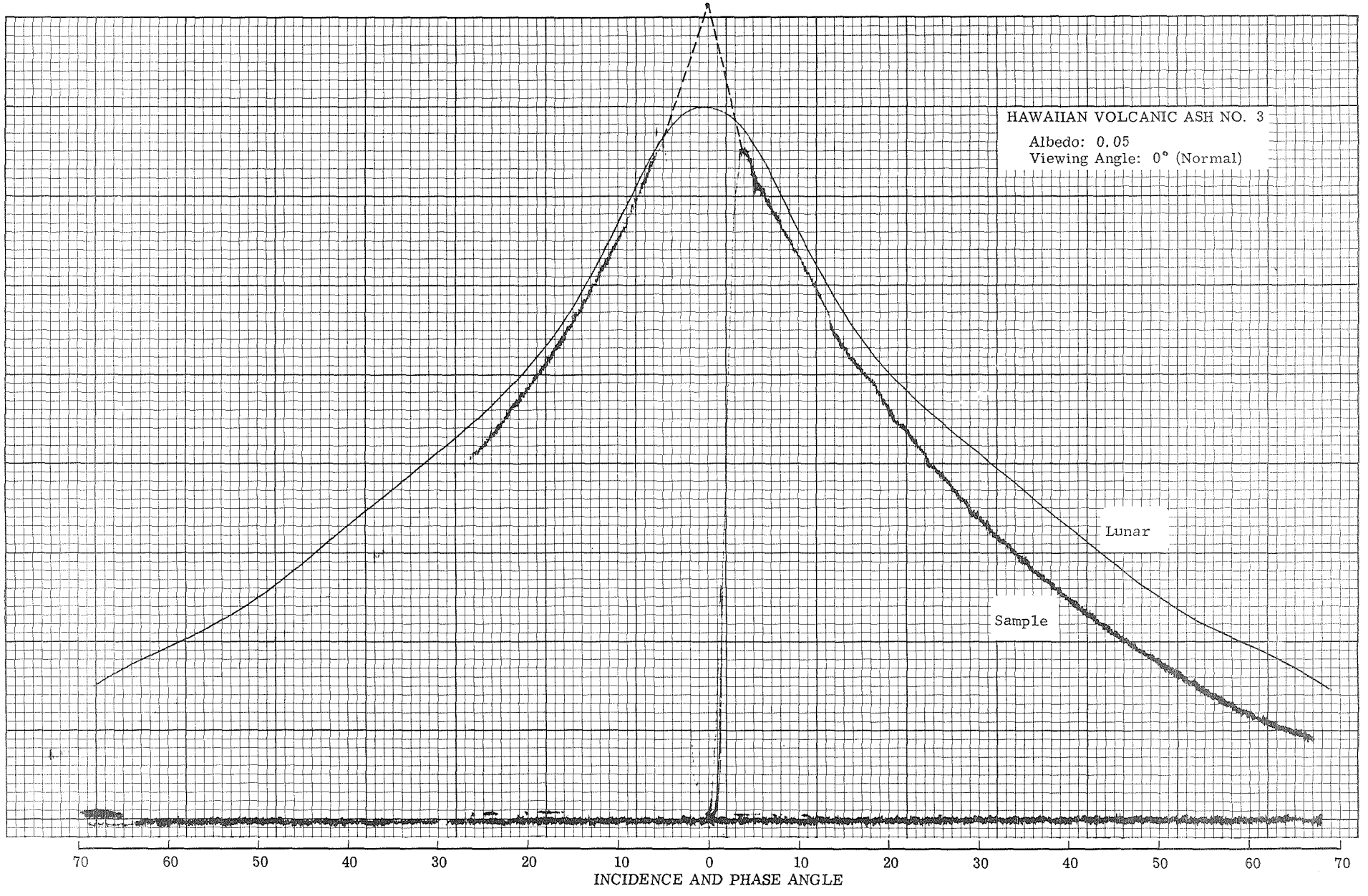
HAWAIIAN VOLCANIC ASH NO. 3
Albedo: 0.05
Viewing Angle: 0° (Normal)
Lunar
Sample
70 60 50 40 30 20 10 0 10 20 30 40 50 60 70
INCIDENCE AND PHASE ANGLE

Figure 7a.

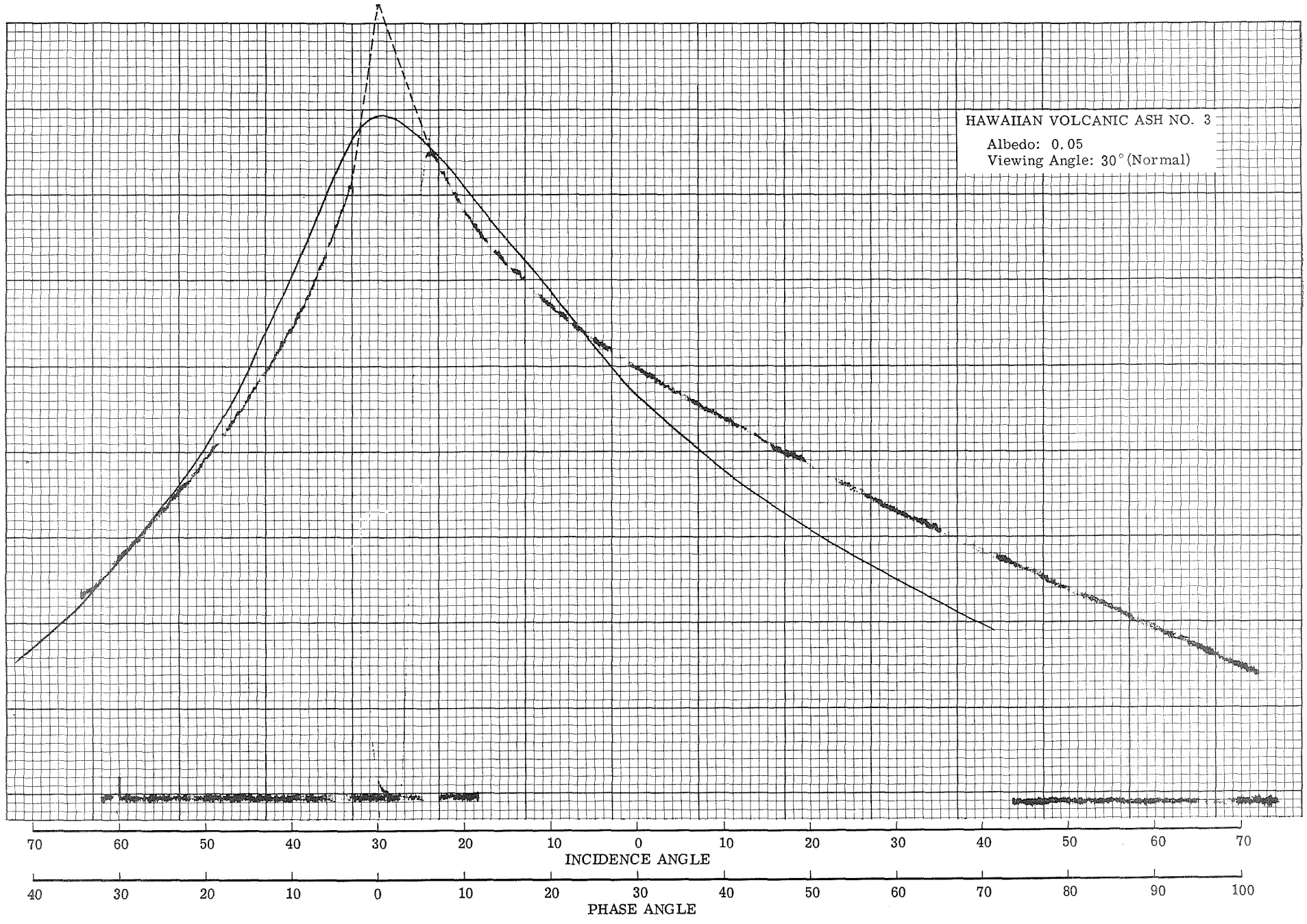
HAWAIIAN VOLCANIC ASH NO. 3
Albedo: 0.05
Viewing Angle: 30° (Normal)
70 60 50 40 30 20 10 0 10 20 30 40 50 60 70
INCIDENCE ANGLE
40 30 20 10 0 10 20 30 40 50 60 70 80 90 100
PHASE ANGLE

Figure 7b.

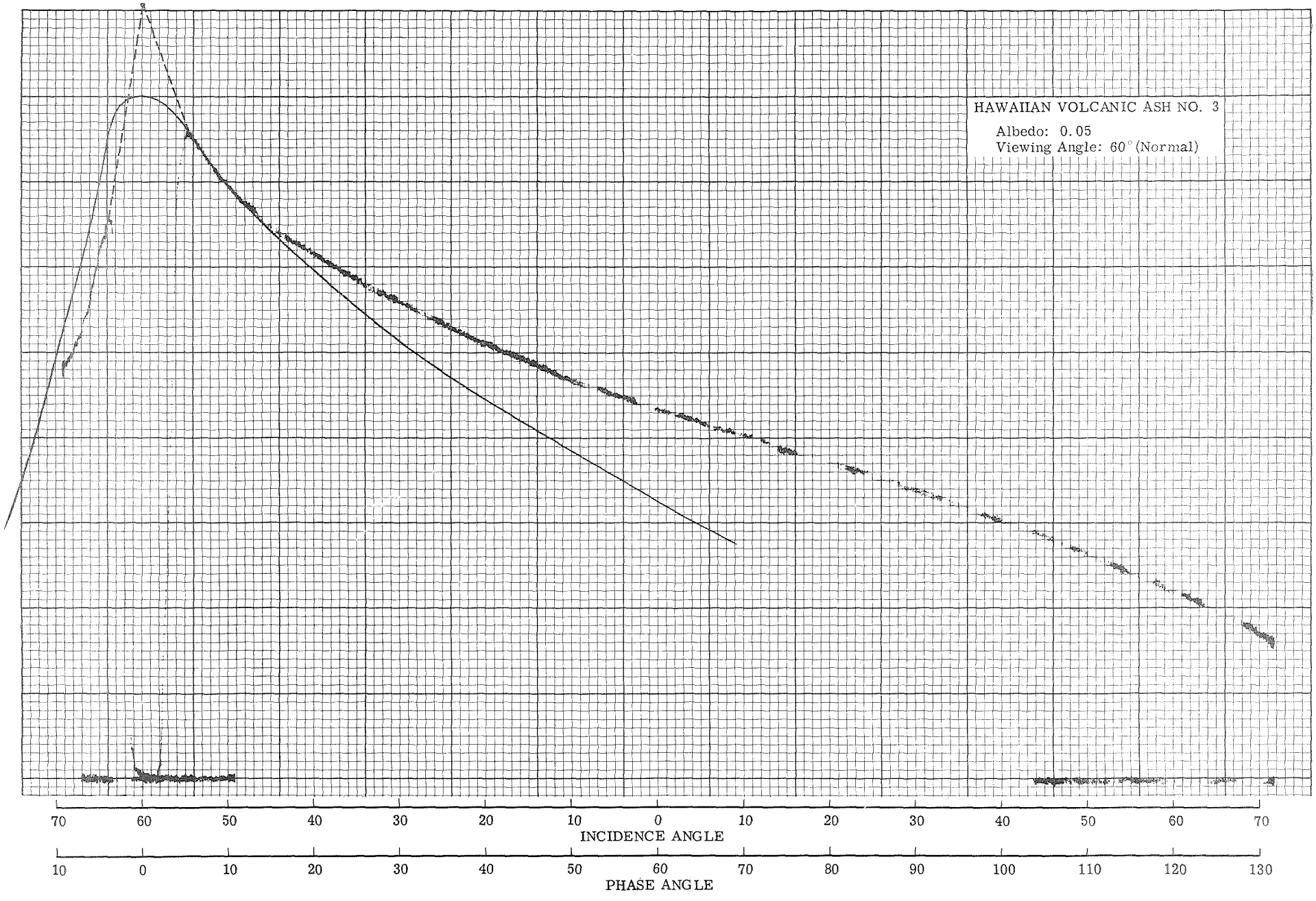
HAWAIIAN VOLCANIC ASH NO. 3
Albedo: 0.05
Viewing Angle: 60° (Normal)
70 60 50 40 30 20 10 0 10 20 30 40 50 60 70
INCIDENCE ANGLE
10 0 10 20 30 40 50 60 70 80 90 100 110 120 130
PHASE ANGLE

Figure 7c.

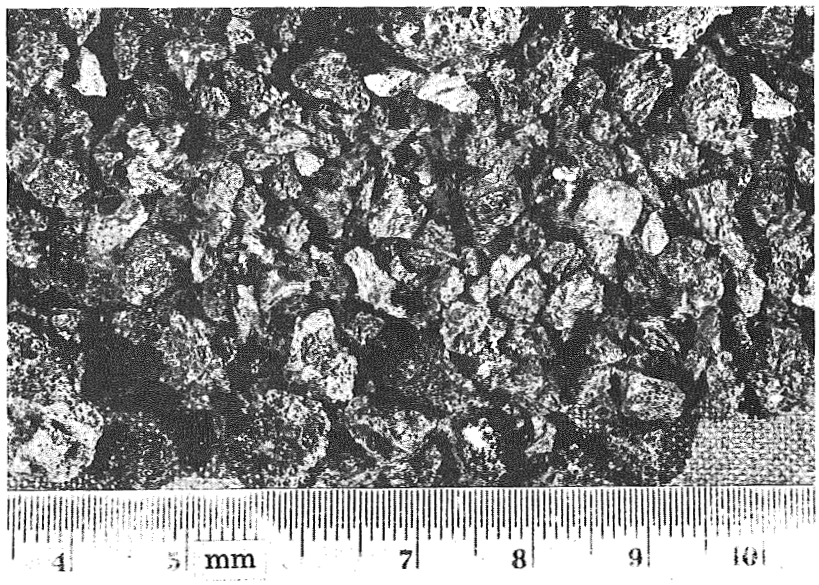

Figure 7d. Volcanic Ash Sample No. 3

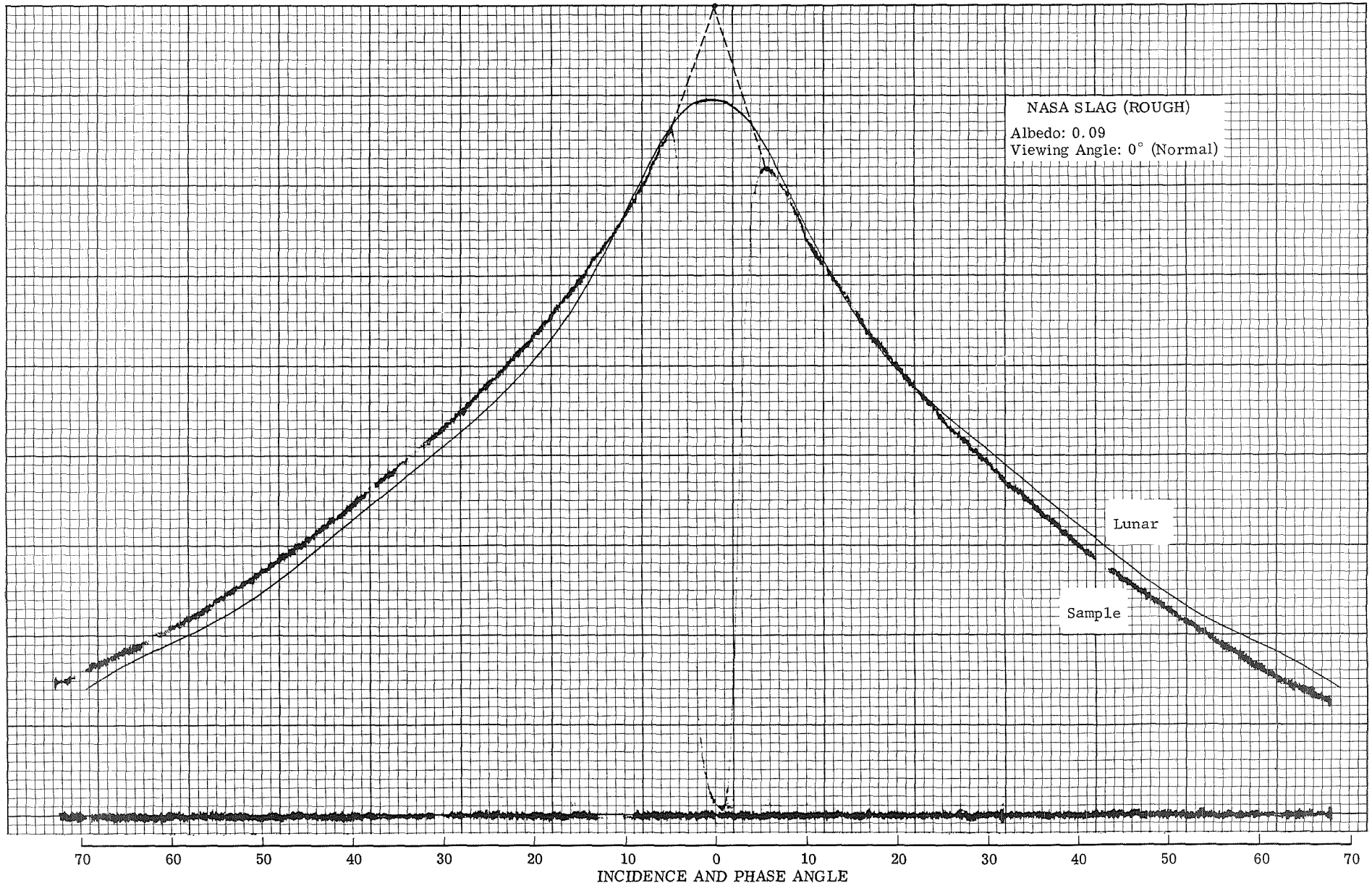
NASA SLAG (ROUGH)
Albedo: 0.09
Viewing Angle: 0° (Normal)
Lunar
Sample
70
60
50
40
30
20
10
0
10
20
30
40
50
60
70
INCIDENCE AND PHASE ANGLE

Figure 8a.

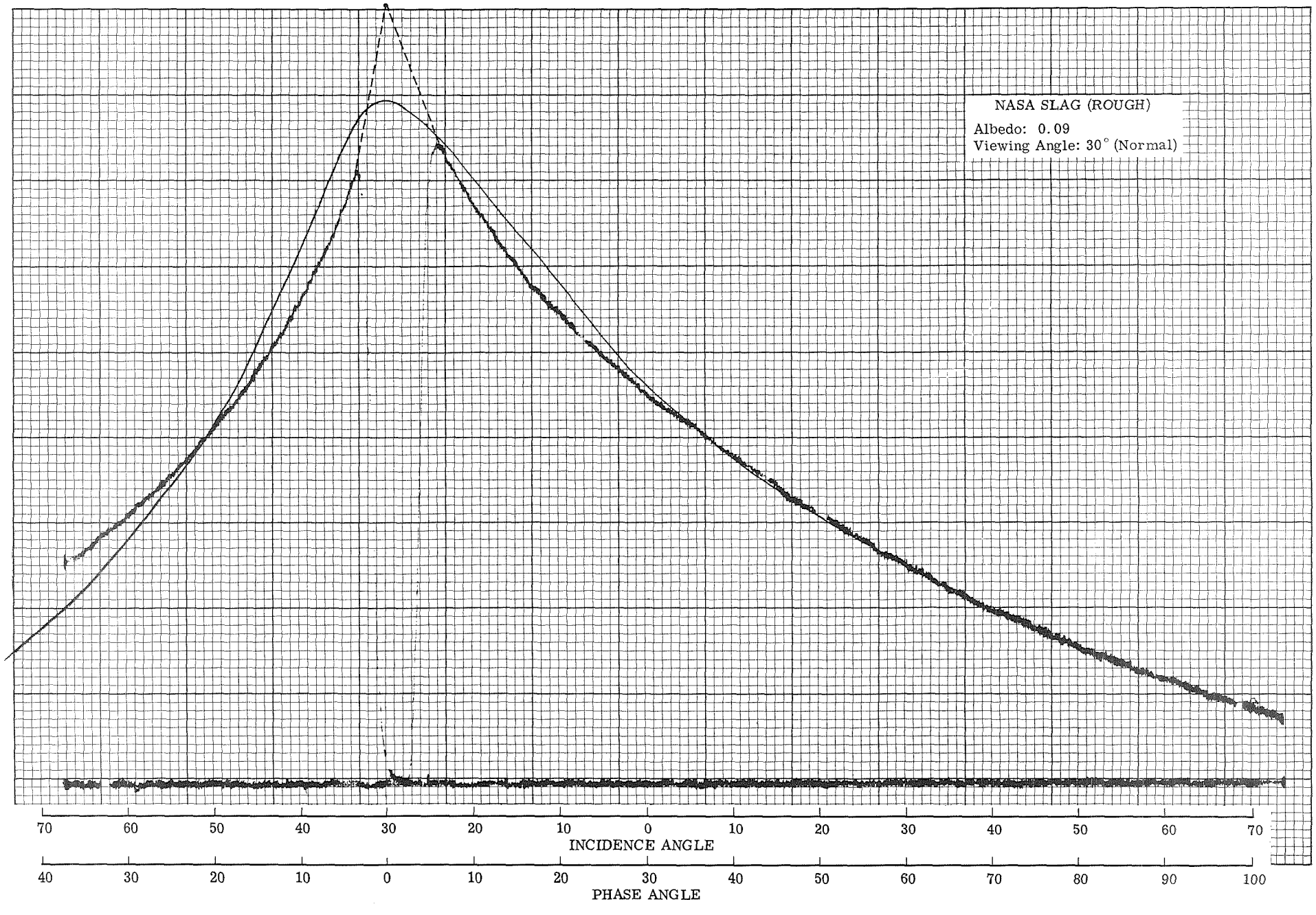

Figure 8b.

Research Dept.
RM-250
November 1964

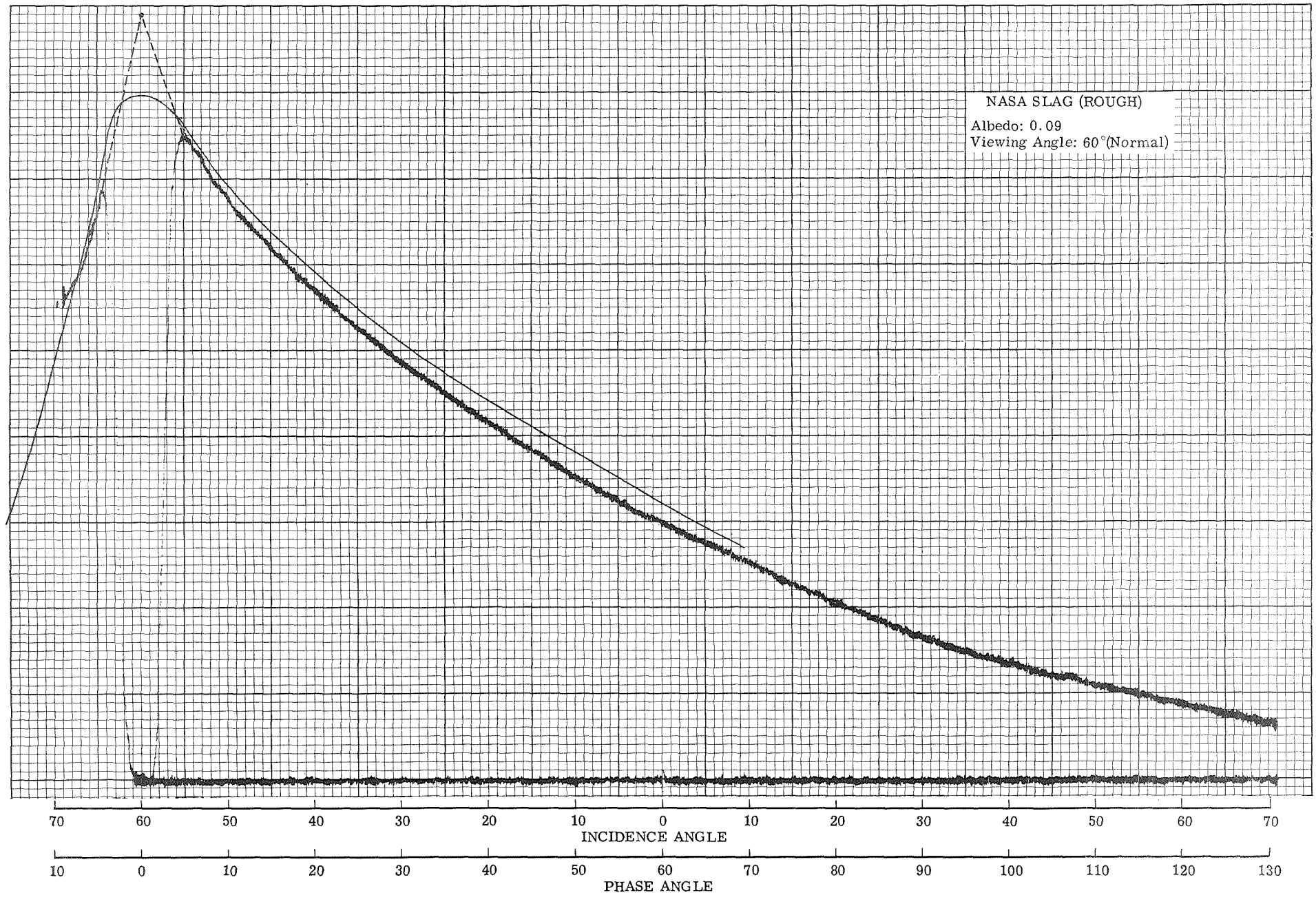
NASA SLAG (ROUGH)
Albedo: 0.09
Viewing Angle: 60°(Normal)
70 60 50 40 30 20 10 0 10 20 30 40 50 60 70
INCIDENCE ANGLE
10 0 10 20 30 40 50 60 70 80 90 100 110 120 130
PHASE ANGLE

Figure 8c.

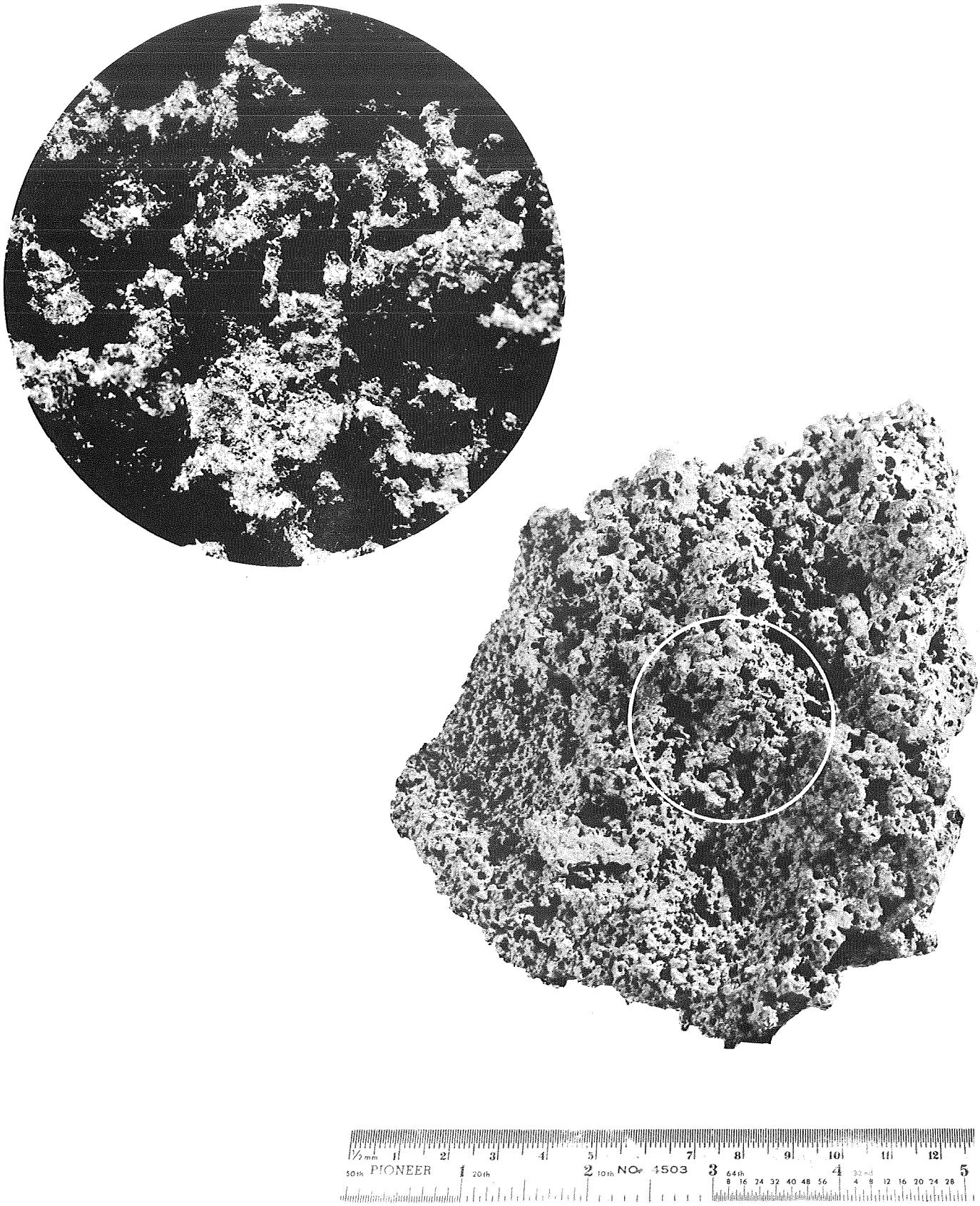

Figure 8d. NASA Slag

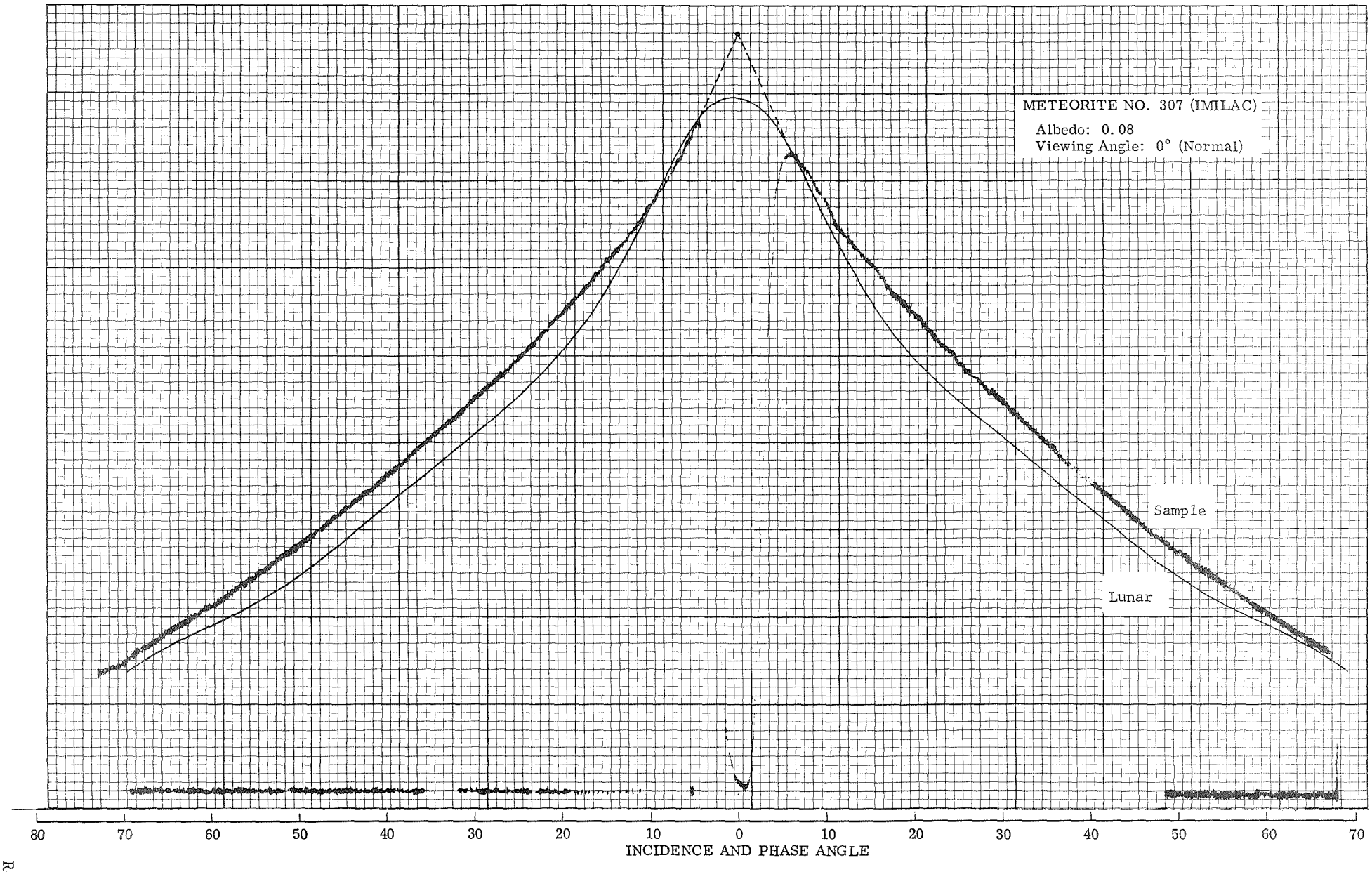
METEORITE NO. 307 (IMILAC)
Albedo: 0.08
Viewing Angle: 0° (Normal)
Sample
Lunar
80
70
60
50
40
30
20
10
0
10
20
30
40
50
60
70
INCIDENCE AND PHASE ANGLE

Figure 9a.

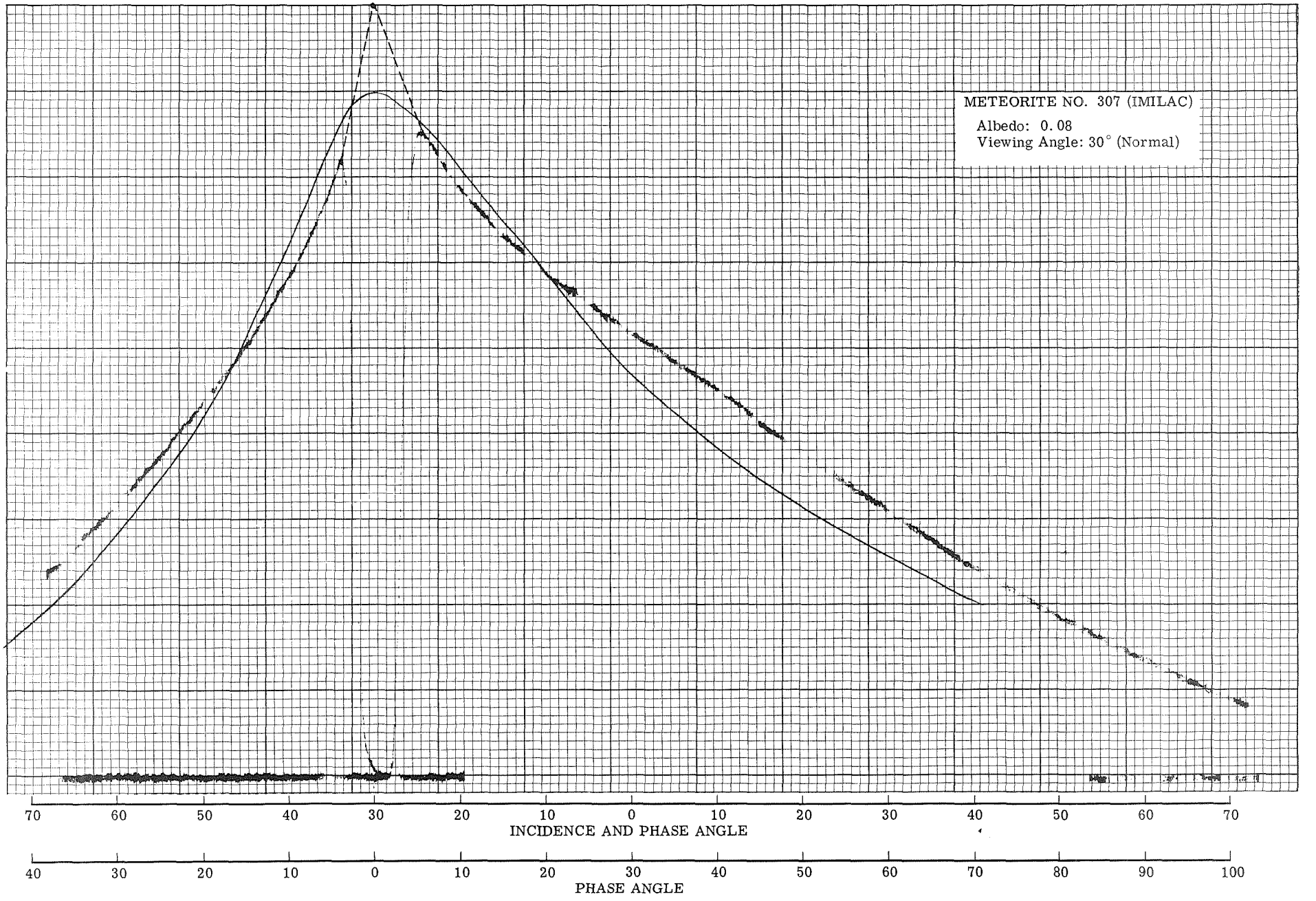

Figure 9b.

Research Dept.
RM-250
November 1964

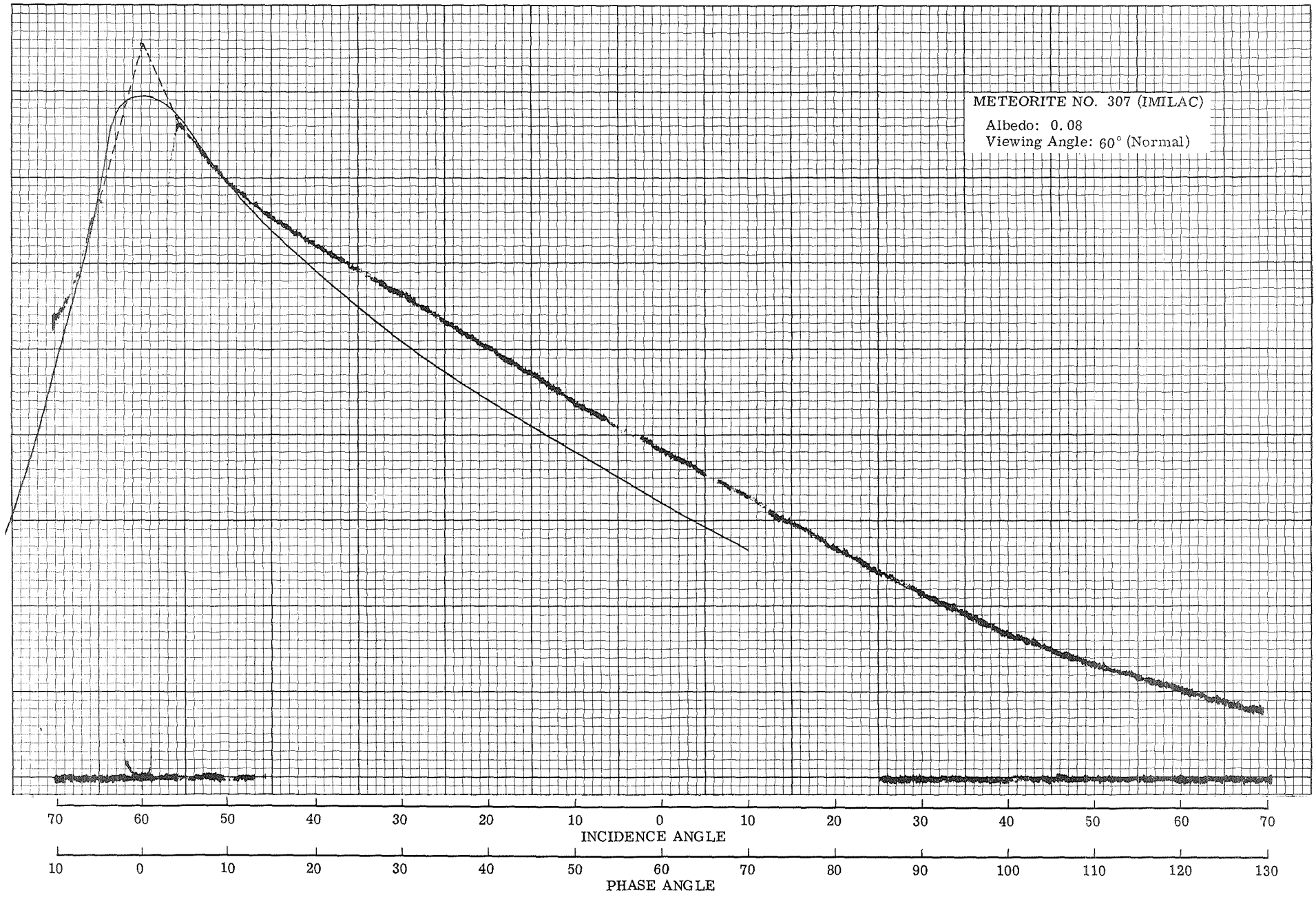
METEORITE NO. 307 (IMILAC)
Albedo: 0.08
Viewing Angle: 60° (Normal)
70 60 50 40 30 20 10 0 10 20 30 40 50 60 70
INCIDENCE ANGLE
10 0 10 20 30 40 50 60 70 80 90 100 110 120 130
PHASE ANGLE

Figure 9c.

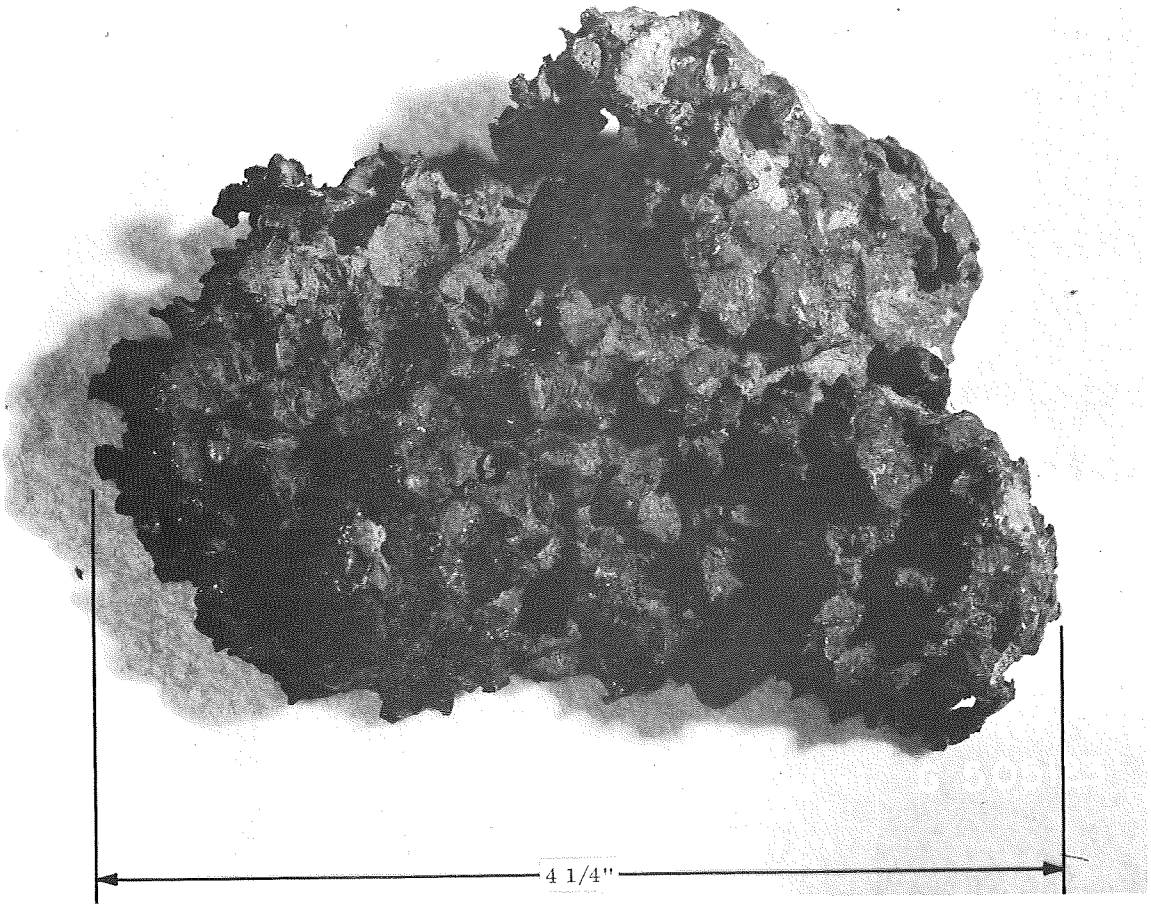

Figure 9d. "Imilac" Metallic Meteorite

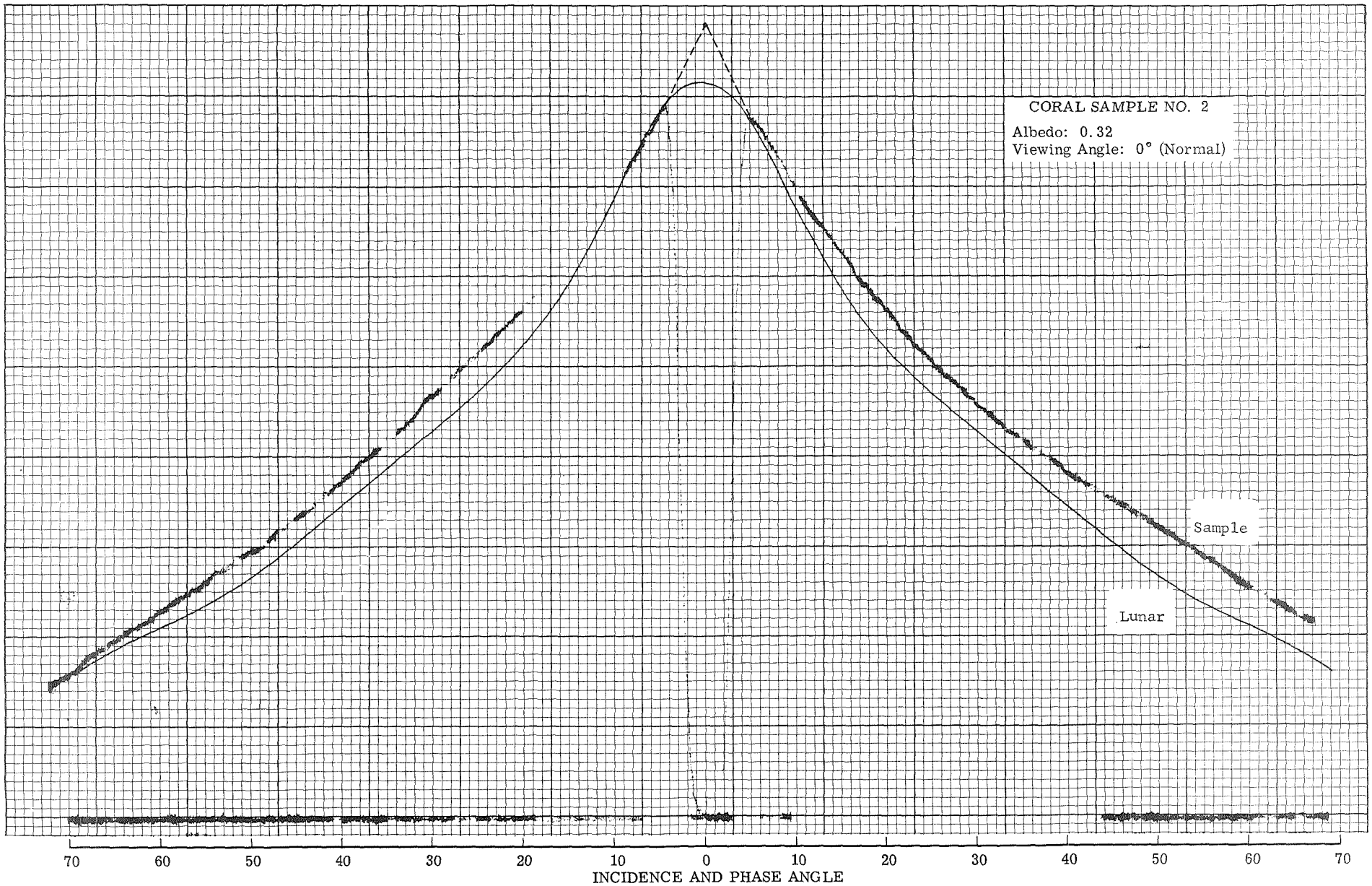
CORAL SAMPLE NO. 2
Albedo: 0.32
Viewing Angle: 0° (Normal)
Sample
Lunar
70
60
50
40
30
20
10
0
10
20
30
40
50
60
70
INCIDENCE AND PHASE ANGLE

Figure 10a.

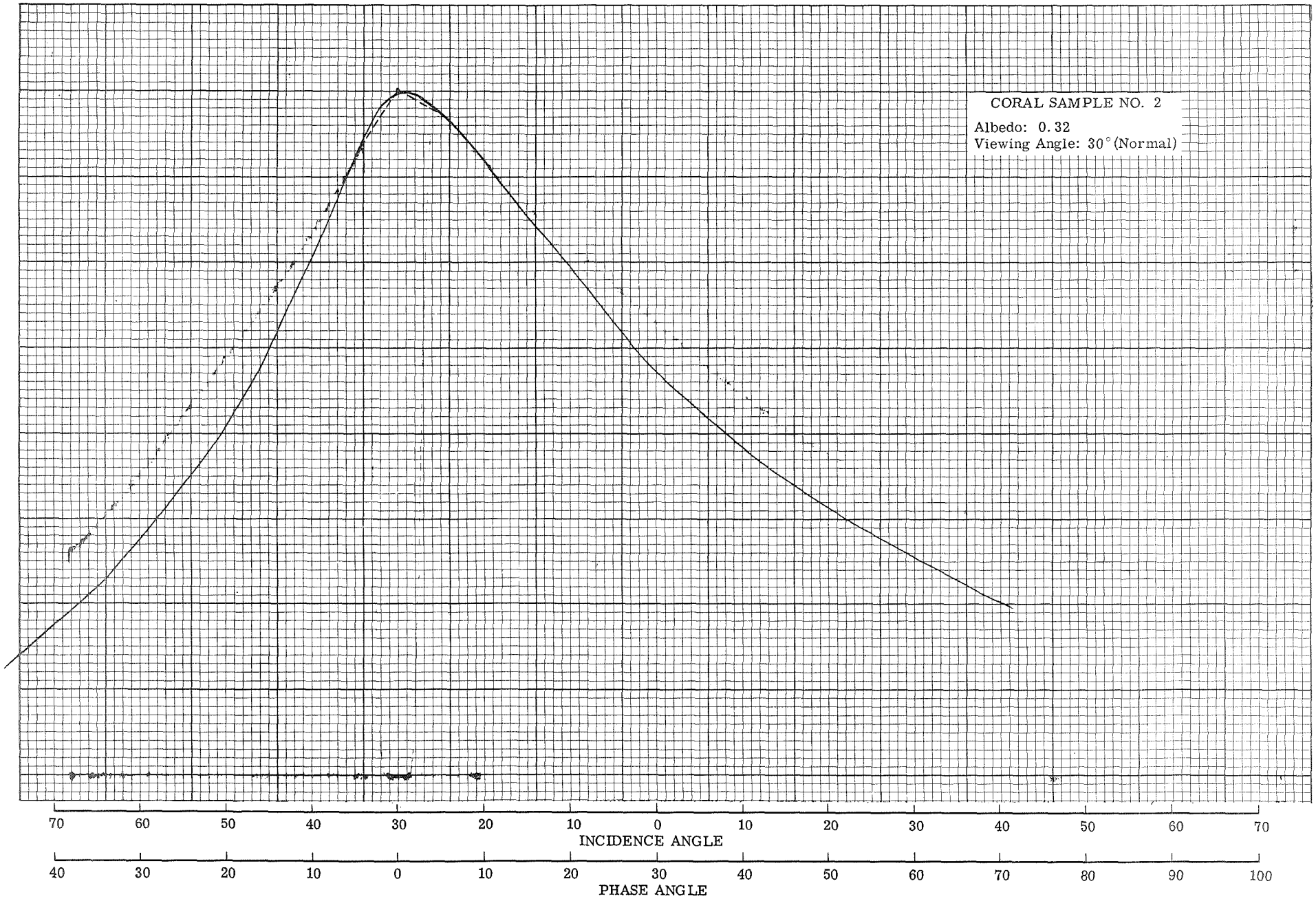
CORAL SAMPLE NO. 2
Albedo: 0.32
Viewing Angle: 30° (Normal)
70 60 50 40 30 20 10 0 10 20 30 40 50 60 70
INCIDENCE ANGLE
40 30 20 10 0 10 20 30 40 50 60 70 80 90 100
PHASE ANGLE

Figure 10b.

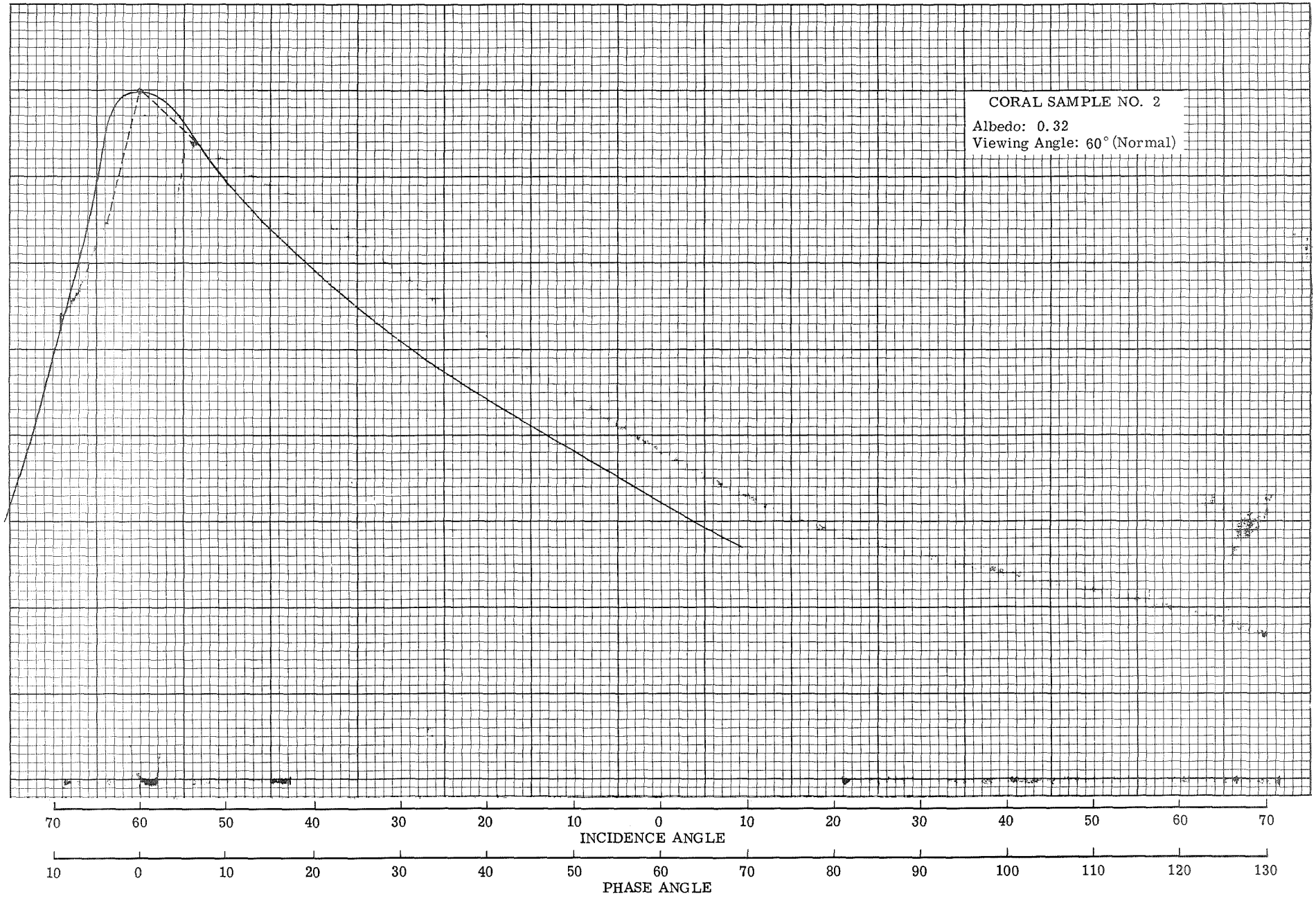
CORAL SAMPLE NO. 2
Albedo: 0.32
Viewing Angle: 60° (Normal)
70 60 50 40 30 20 10 0 10 20 30 40 50 60 70
INCIDENCE ANGLE
10 0 10 20 30 40 50 60 70 80 90 100 110 120 130
PHASE ANGLE

Figure 10c.

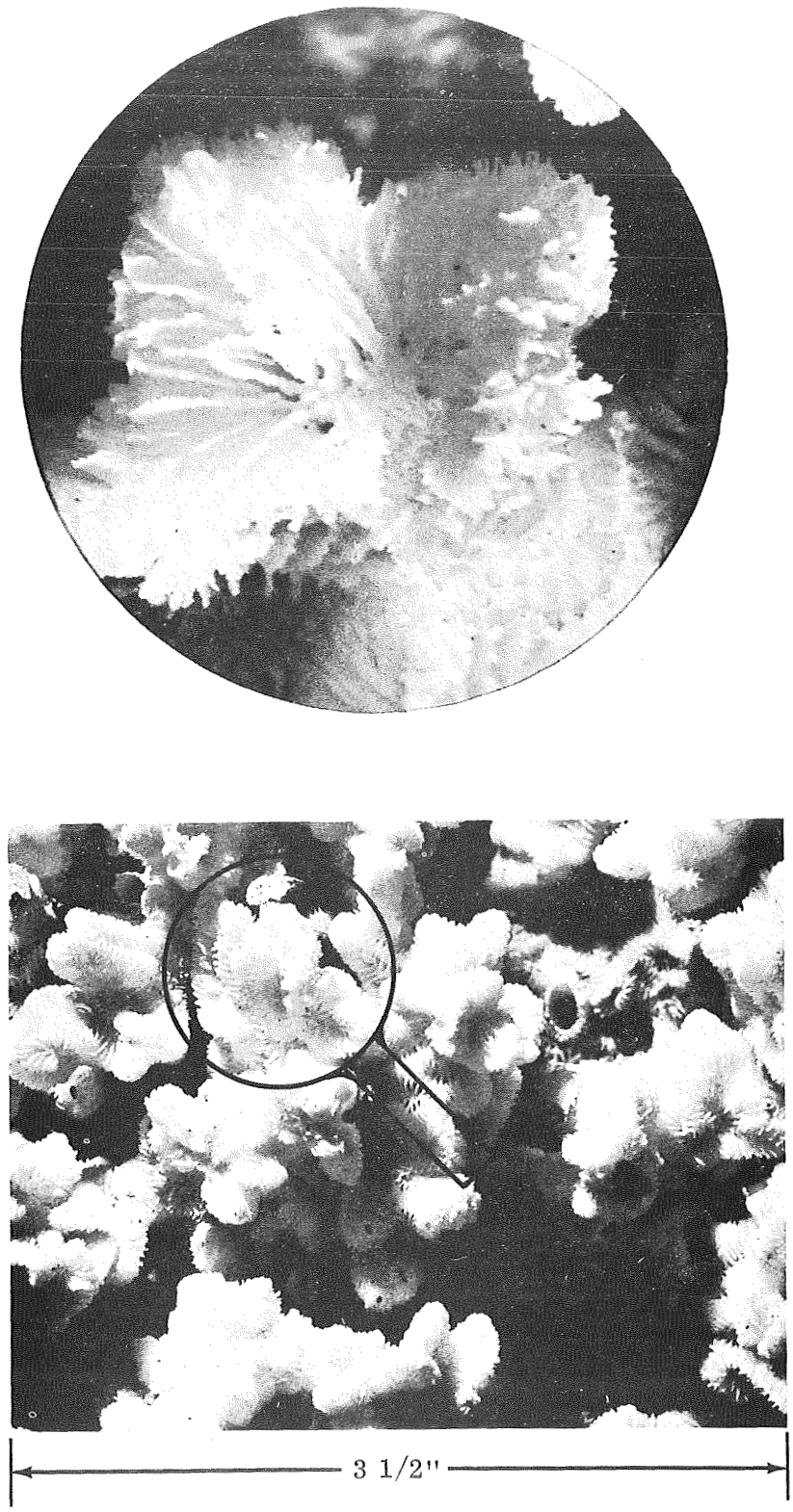

Figure 10d. Caribbean Coral Sample No. 2

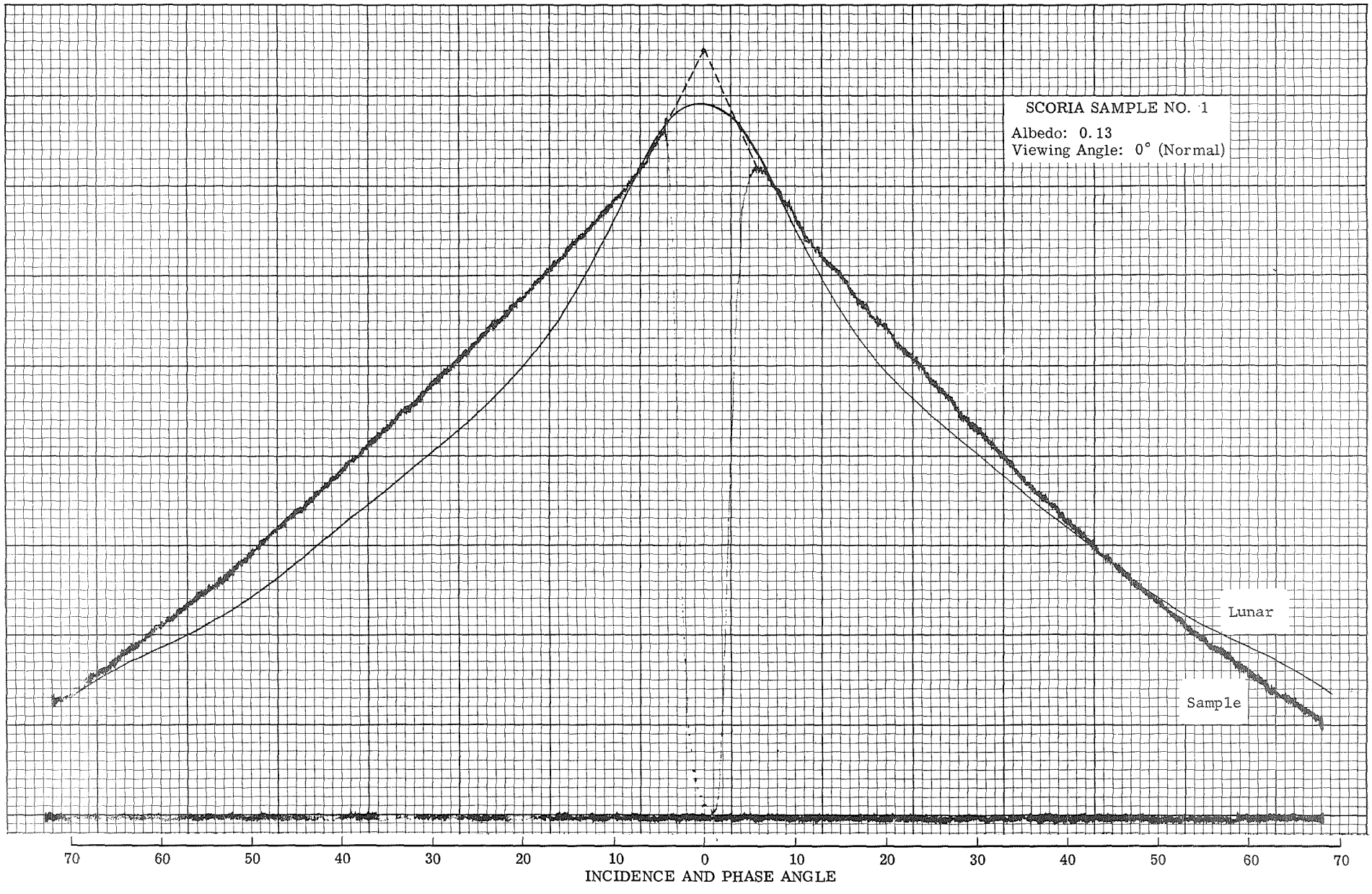
SCORIA SAMPLE NO. 1
Albedo: 0.13
Viewing Angle: 0° (Normal)
Lunar
Sample
70
60
50
40
30
20
10
0
10
20
30
40
50
60
70
INCIDENCE AND PHASE ANGLE

Figure 11a.

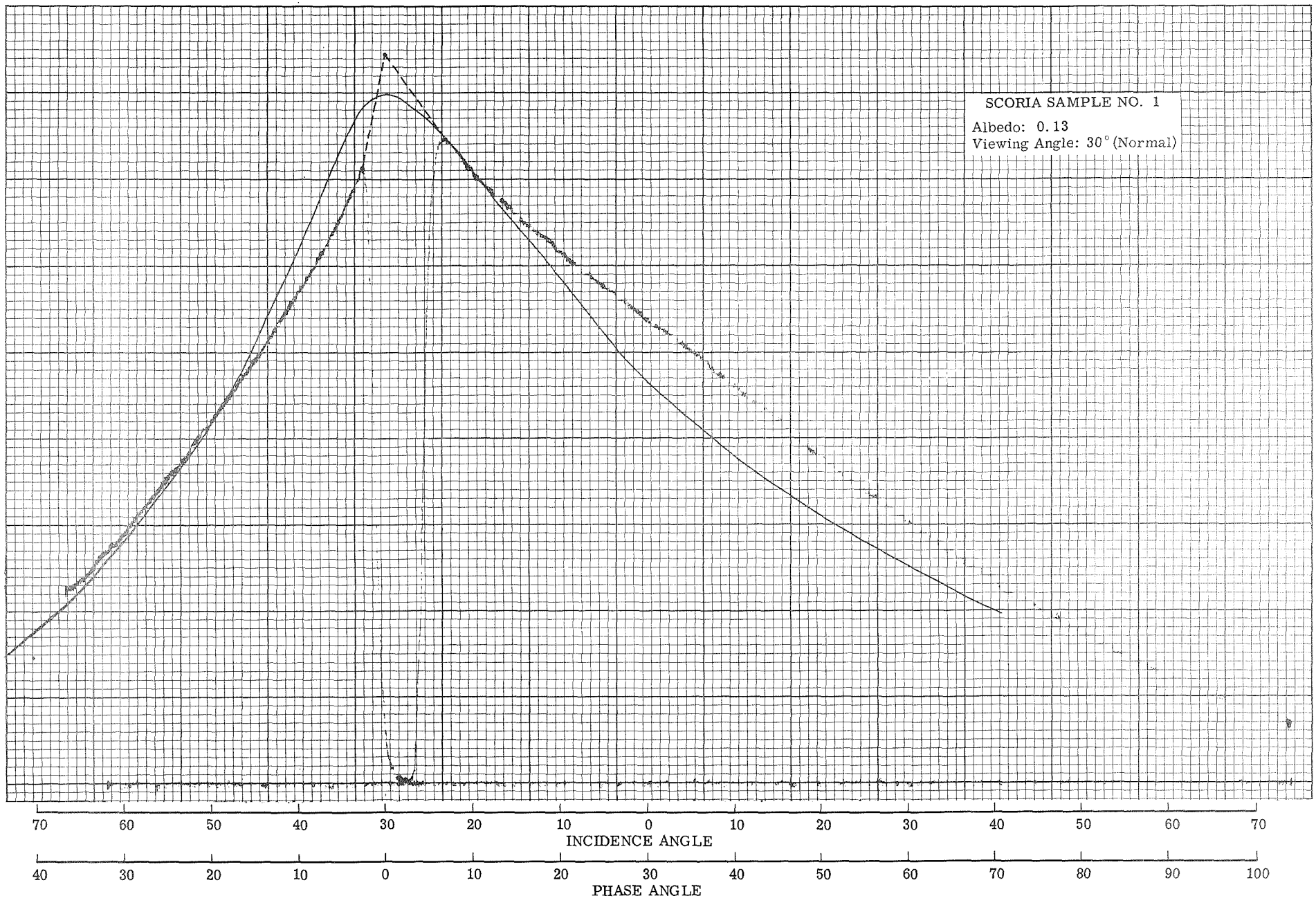

Figure 11b.

Research Dept.
RM-250
November 1964

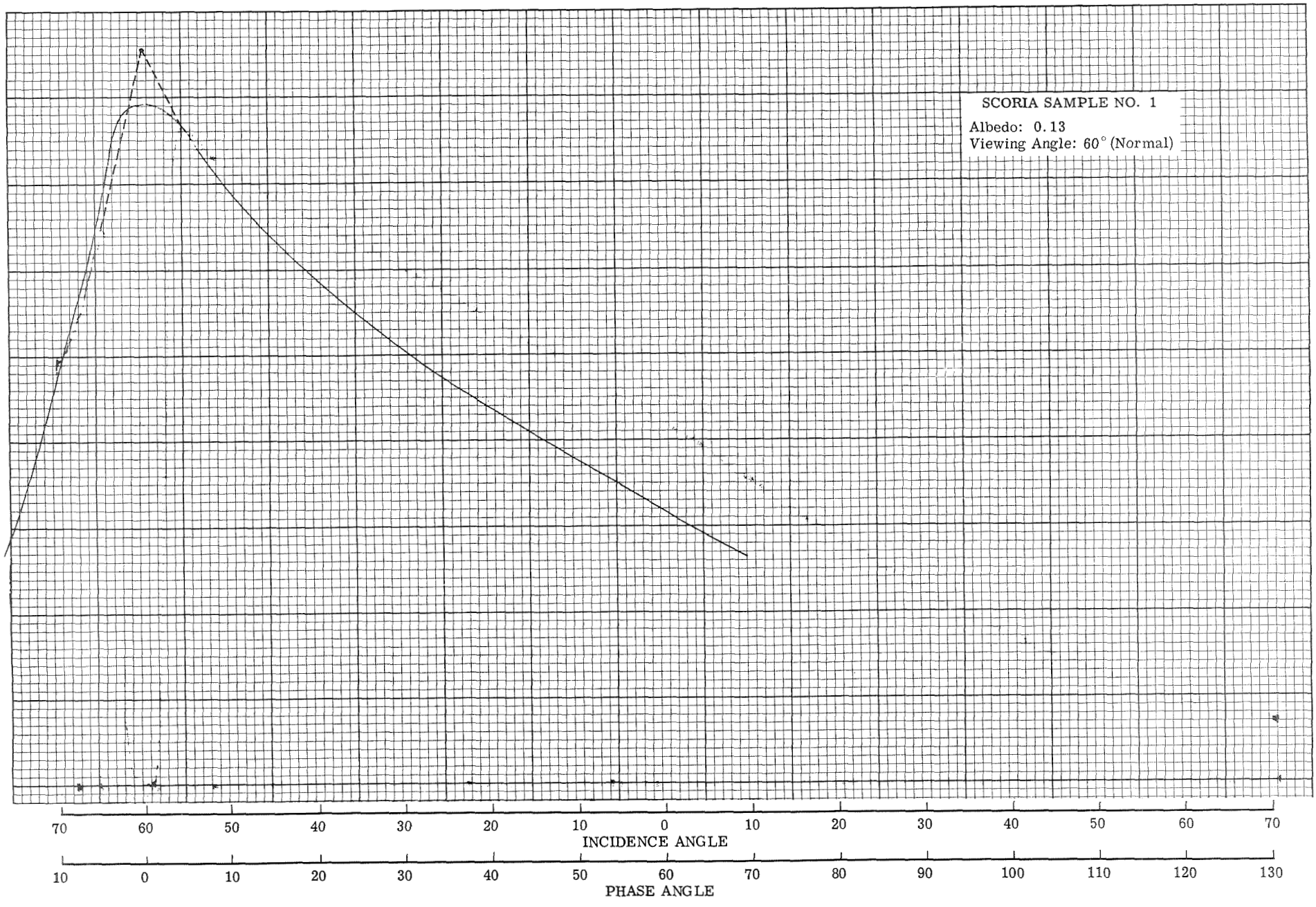
SCORIA SAMPLE NO. 1
Albedo: 0.13
Viewing Angle: 60° (Normal)
70 60 50 40 30 20 10 0 10 20 30 40 50 60 70
INCIDENCE ANGLE
10 0 10 20 30 40 50 60 70 80 90 100 110 120 130
PHASE ANGLE

Figure 11c.

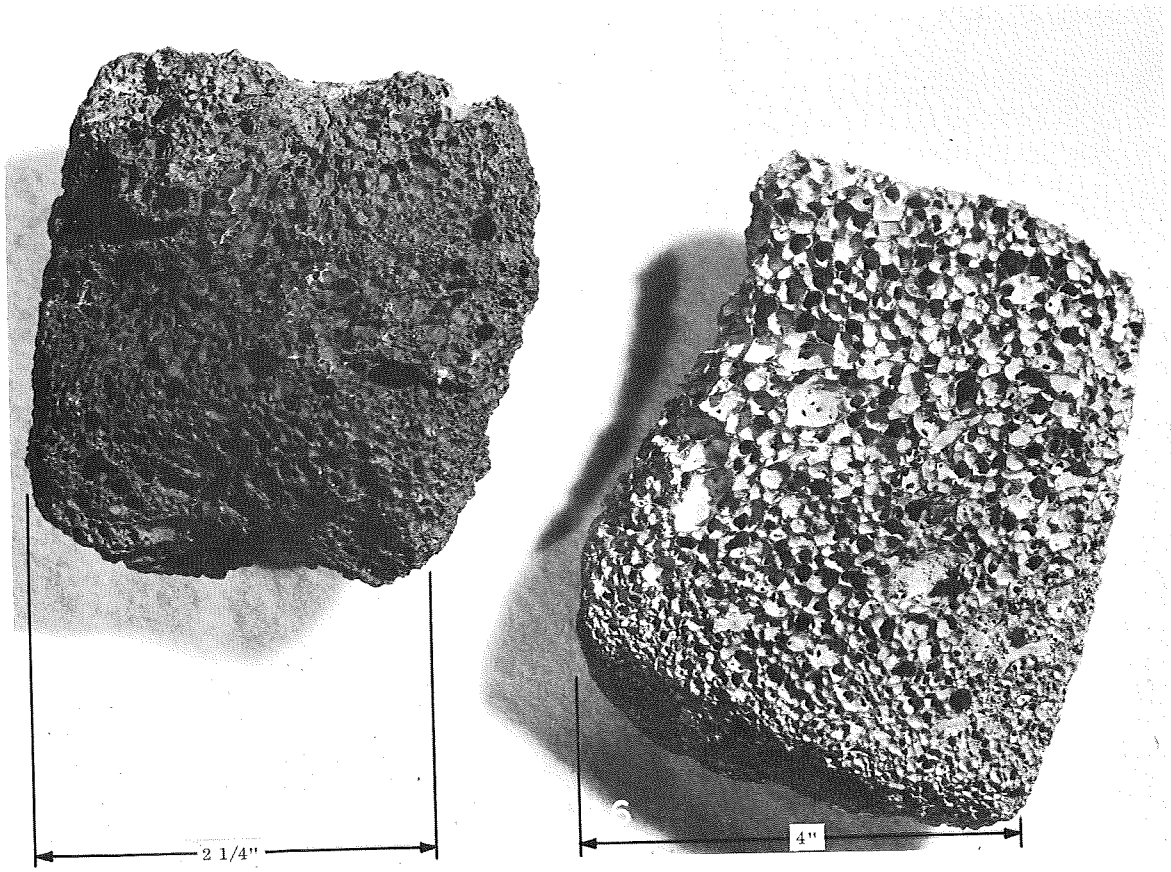

Figure 11d. Scoria No. 1 (Light) and No. 2 (Dark)

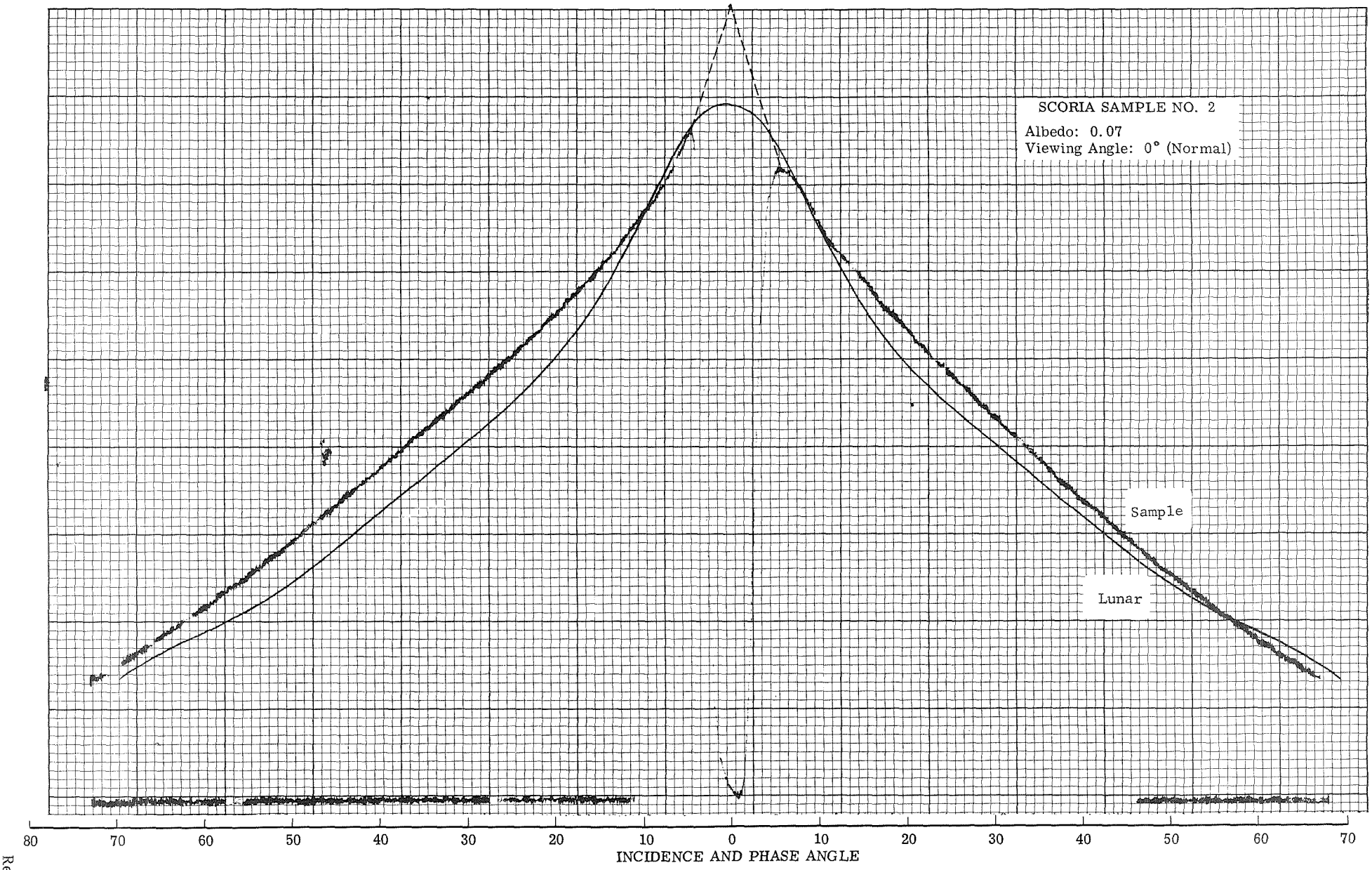
SCORIA SAMPLE NO. 2
Albedo: 0.07
Viewing Angle: 0° (Normal)
Sample
Lunar
80
70
60
50
40
30
20
10
0
10
20
30
40
50
60
70
INCIDENCE AND PHASE ANGLE

Figure 12a.

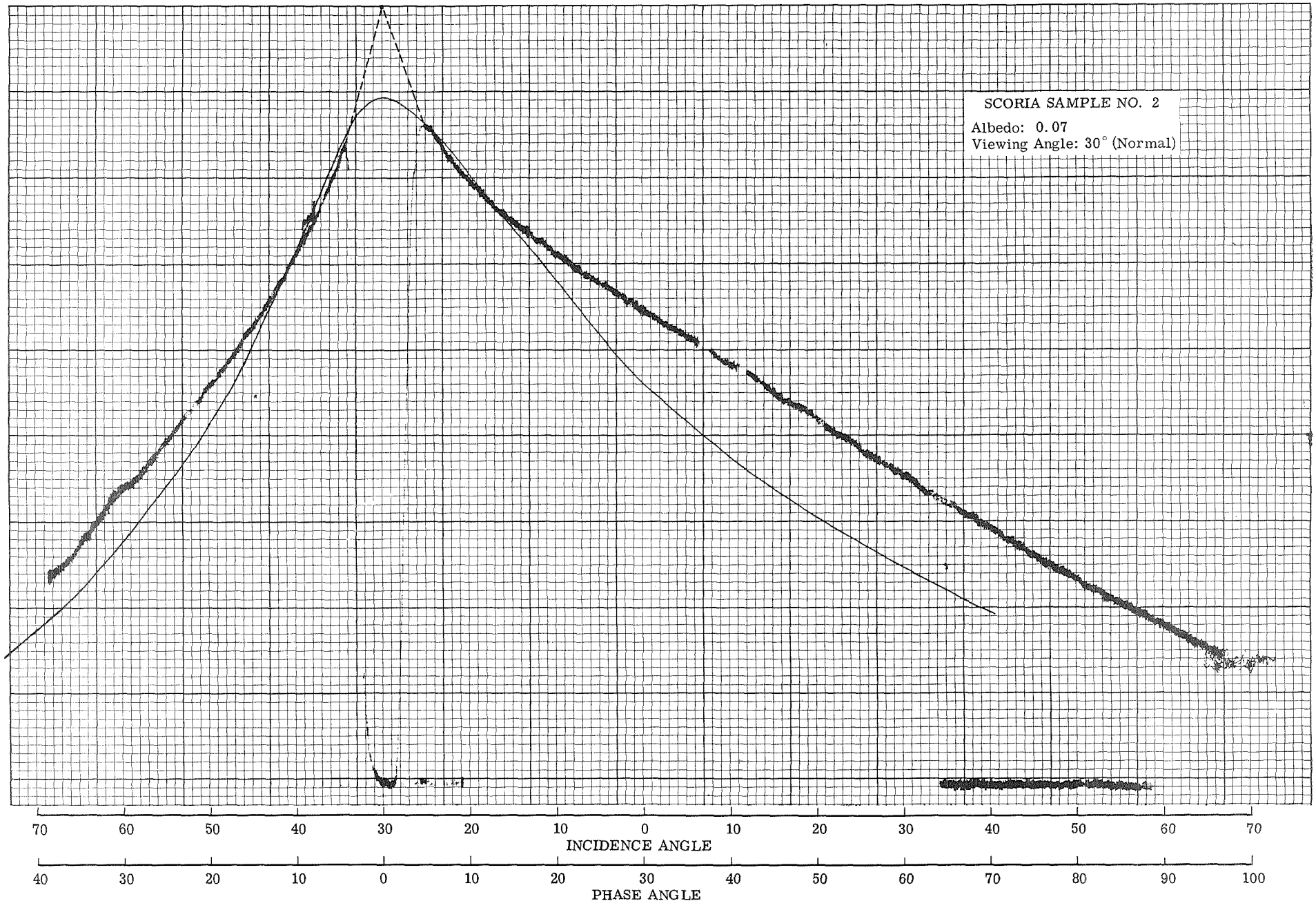

Figure 12b.

Research Dept.
RM-250
November 1964

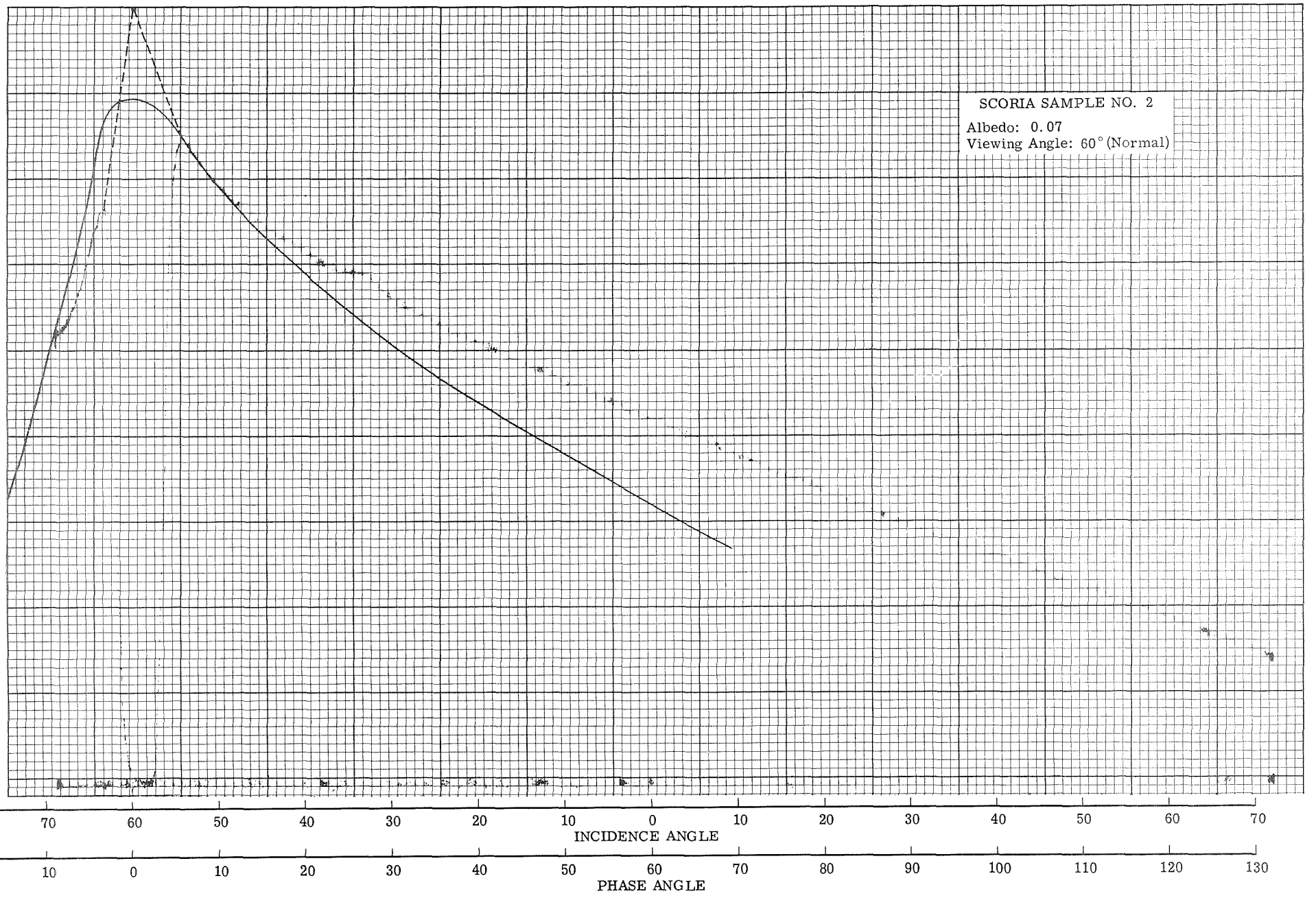

Figure 12c.

Research Dept.
RM-250
November 1964

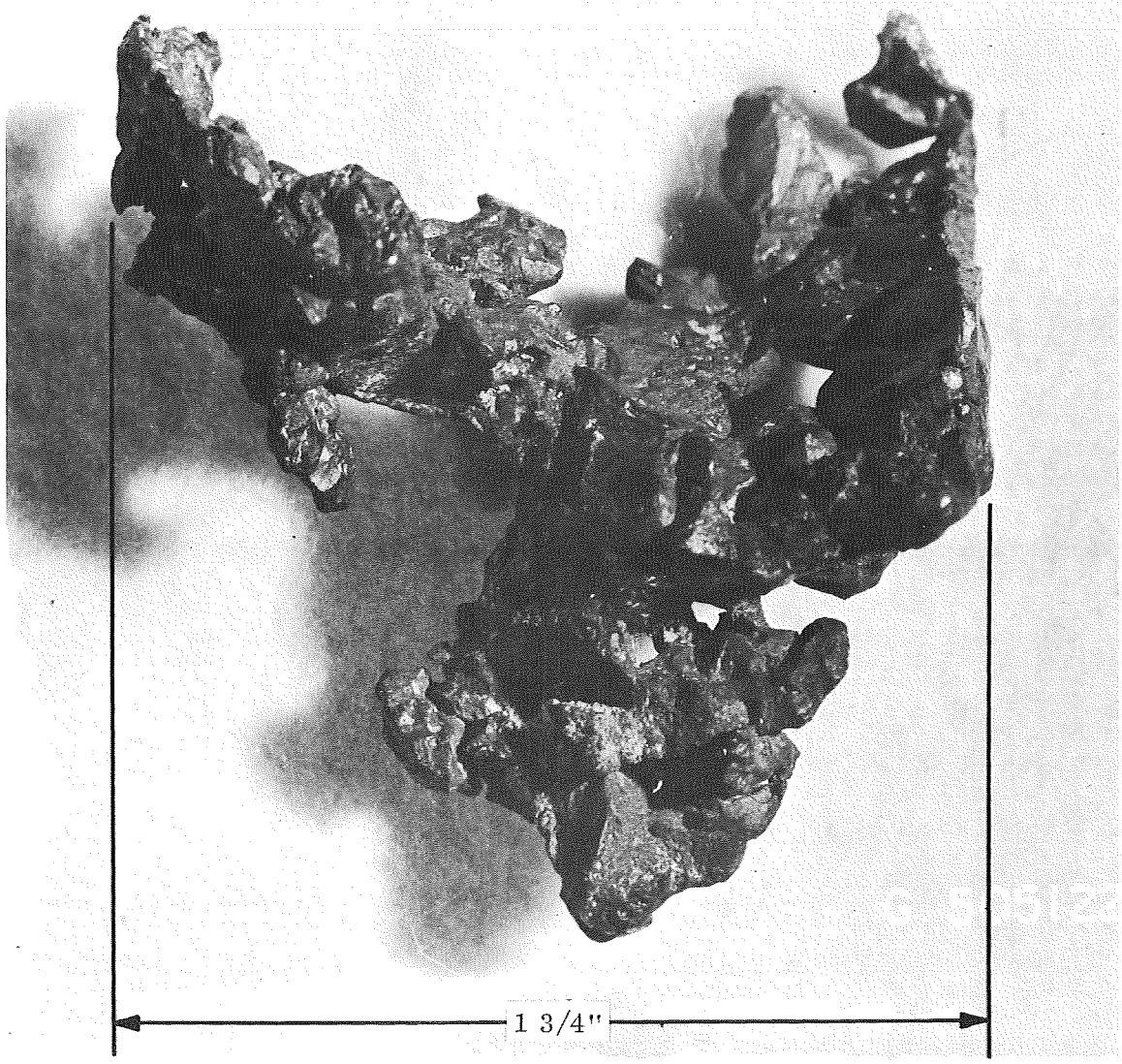

Figure 13. Native Copper

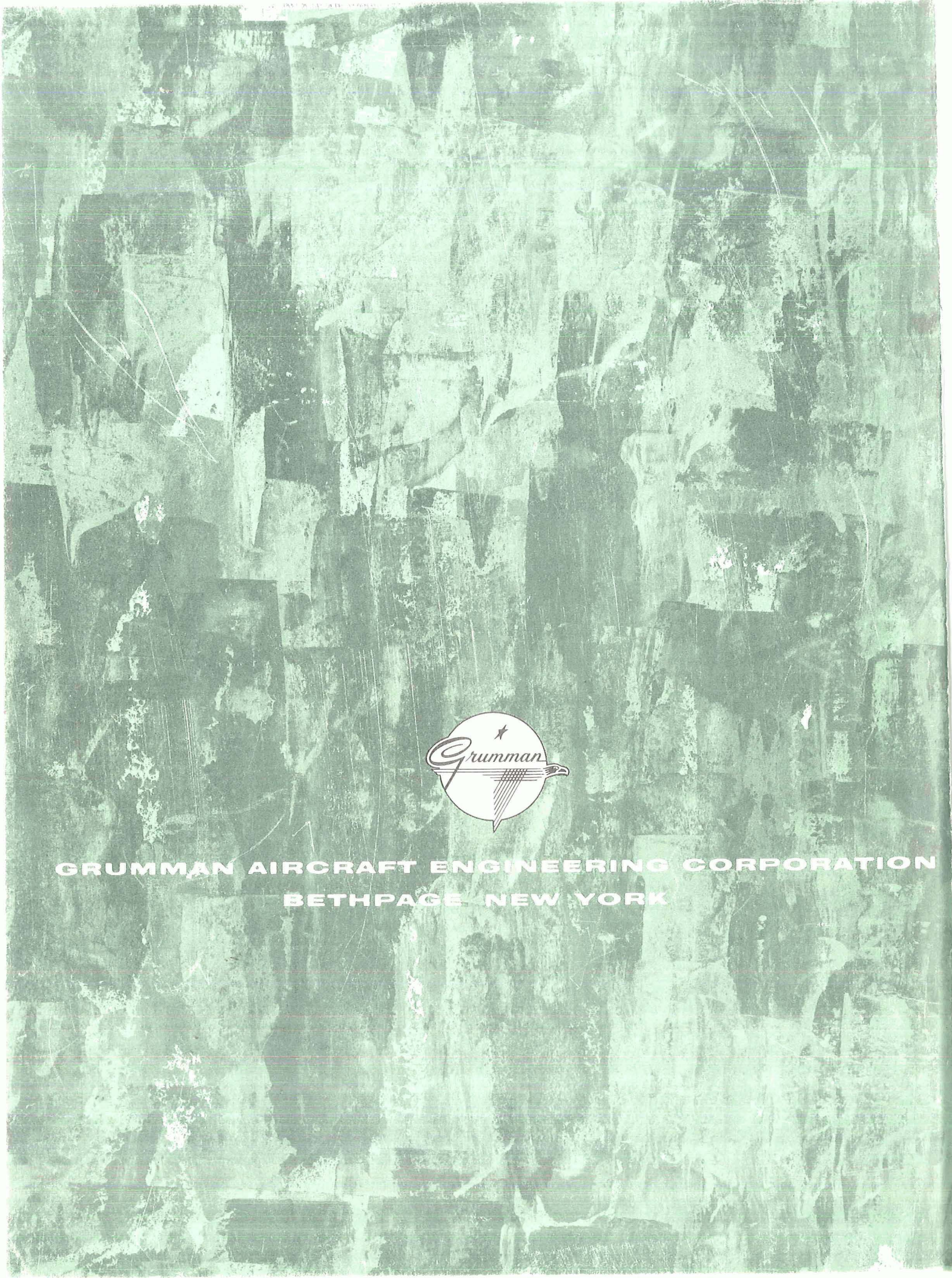

GRUMMAN AIRCRAFT ENGINEERING CORPORATION

BETHPAGE NEW YORK